

ADAPTIVE PARAMETER OPTIMIZATION FOR AN ELLIPTIC-PARABOLIC SYSTEM USING THE REDUCED-BASIS METHOD WITH HIERARCHICAL A-POSTERIORI ERROR ANALYSIS ^{*,**}

BEHZAD AZMI¹, ANDREA PETROCCHI¹ AND STEFAN VOLKWEIN¹

Abstract. In this paper the authors study a non-linear elliptic-parabolic system, which is motivated by mathematical models for lithium-ion batteries. One state satisfies a parabolic reaction diffusion equation and the other one an elliptic equation. The goal is to determine several scalar parameters in the coupled model in an optimal manner by utilizing a reliable reduced-order approach based on the reduced basis (RB) method. However, the states are coupled through a strongly non-linear function, and this makes the evaluation of online-efficient error estimates difficult. First the well-posedness of the system is proved. Then a Galerkin finite element and RB discretization are described for the coupled system. To certify the RB scheme hierarchical a-posteriori error estimators are utilized in an adaptive trust-region optimization method. Numerical experiments illustrate good approximation properties and efficiencies by using only a relatively small number of reduced basis functions.

2020 Mathematics Subject Classification. 65K10, 65M20, 49M41.

August 2, 2023.

1. INTRODUCTION

The modelling of lithium-ion batteries has received an increasing amount of attention in the recent past. Several companies worldwide are developing such batteries for consumer electronic applications, in particular, for electric-vehicle applications. To achieve the performance and lifetime demands in this area, exact mathematical models of the battery are required. Moreover, the multiple evaluations of the battery model for different parameter settings involve a large amount of time and experimental effort. Here, the derivation of reliable mathematical models and their efficient numerical realization are very important issues in order to reduce both computational time and cost in the improvement of the performance of batteries.

Mathematical models for lithium-ion batteries describe the evolution of lithium-ion concentration in the different regions of a battery and the electric potentials in the so-called electrolyte and solid phases. We refer to [33], where the transport processes are described by a coupled system of partial differential equations (PDEs).

Keywords and phrases: elliptic and parabolic partial differential equations, parameter estimation, reduced-order modelling, hierarchical a-posteriori error estimate, trust-region methods.

* *The authors got partial financial support within the COMET K2 Competence Centers for Excellent Technologies from the Austrian Federal Ministry for Climate Action, the Austrian Federal Ministry for Digital and Economic Affairs, the Province of Styria (Dept. 12) and the Styrian Business Promotion Agency.*

** *The authors furthermore acknowledge funding by the Deutsche Forschungsgemeinschaft for the project Localized Reduced Basis Methods for PDE-constrained Parameter Optimization under contract VO 1658/6-1.*

¹ University of Konstanz, Department of Mathematics and Statistics, Konstanz, 78457 Germany,

e-mail: behzad.azmi@uni-konstanz.de & andrea.petrocchi@uni-konstanz.de & stefan.volkwein@uni-konstanz.de

The physical and chemical details can be found, e.g., in [27,28]. The equation system models a physico-chemical micro-heterogeneous battery model. A macro-homogeneous approach is developed in the pioneering work [30] and forms the basis for further investigations; cf. [12,15,17,37,41], for instance. Well-posedness is studied, e.g., in [40,44].

The goal of the present work is to make a first step in order to extend the theoretical and numerical results obtained in [32] to a more realistic battery model. For that purpose, we consider the following still simplified coupled system of parametrized elliptic-parabolic equations

$$y_t(t, x) - \mu_1(\kappa_1(x)y_x(t, x))_x - \mu_2 f(y(t, x), q(t, x)) = 0 \quad \text{f.a.a. } (t, x) \in Q_T, \quad (1a)$$

$$-\mu_3(\kappa_2(x)q_x(t, x))_x + \mu_4 f(y(t, x), q(t, x)) = 0 \quad \text{f.a.a. } (t, x) \in Q_T \quad (1b)$$

together with an initial condition for y , homogeneous Neumann boundary conditions for y and inhomogeneous mixed boundary conditions for q . Throughout we write ‘f.a.a.’ for ‘for almost all’. In (1) the non-linear mapping $f : \mathbb{R}_+ \times \mathbb{R} \rightarrow \mathbb{R}$ has the specific form

$$f(y, q) := \sqrt{y} \sinh(q) \quad \text{for } y \in \mathbb{R}_\geq := \{s \in \mathbb{R} \mid s \geq 0\} \text{ and } q \in \mathbb{R},$$

which is motivated by mathematical models for lithium-ion batteries. There are parameters $\boldsymbol{\mu} = (\mu_i)_{1 \leq i \leq 4} \in \mathbb{R}^4$ in the PDE system which are assumed to be unknown a-priori or which cannot be determined experimentally. Hence, efficient numerical algorithms are needed to estimate these parameters. For this purpose, a parameter identification problem is formulated as a non-linear least squares problem. To speed-up the optimization method a reduced-basis (RB) scheme is used; see, e.g., [22,36] and [26,29,31,43] for battery models. In particular, we apply an adaptive trust-region method that does not need any a-priori computation of an RB subspace on an offline phase, but builds the RB approximation online based on computable a-posteriori error estimates; see [3,4,23,32,34]. Since there are no efficient error bounds available for the non-linear system (1), we utilize hierarchical a-posteriori estimates based on [21].

Summarizing, the new main contributions of the present paper are: (i) proof of existence of a unique weak solution to (1), (ii) extension of the hierarchical error estimation introduced in [21] to a parabolic and non-linear coupled system, (iii) development of a trust-region method for parameter optimization by combining the algorithms in [3,23,34] and the hierarchical error analysis.

The paper is organized as follows: In Section 2 we study the well-posedness and local existence in time of (1). The full- and reduced-order discretization are explained in Section 3. The hierarchical a-posteriori error estimator is derived and tested numerically in Section 4. The parameter estimation is considered in Section 5, where also numerical experiments are presented. Section 6 is devoted to a conclusion. In Appendix A the proofs of Section 2 are given.

2. THE COUPLED ELLIPTIC-PARABOLIC PDE

In this section, we introduce our coupled elliptic-parabolic problem and prove that a unique weak solution exists locally in time.

2.1. The weak formulation

Let $T > 0$ be the (finite) time horizon, $\Omega := (0, L) \subset \mathbb{R}$ be a space interval and let $Q_T := (0, T) \times (0, L)$. We consider the following parameter-dependent parabolic-elliptic coupled system for the two state variables $y, q : Q_T \rightarrow \mathbb{R}$

$$y_t(t, x) - \mu_1(\kappa_1(x)y_x(t, x))_x - \mu_2 f(y(t, x), q(t, x)) = 0 \quad \text{f.a.a. } (t, x) \in Q_T, \quad (2a)$$

$$-\mu_3(\kappa_2(x)q_x(t, x))_x + \mu_4 f(y(t, x), q(t, x)) = 0 \quad \text{f.a.a. } (t, x) \in Q_T \quad (2b)$$

with homogeneous Neumann boundary conditions

$$y_x(t, 0) = y_x(t, L) = 0 \quad \text{f.a.a. } t \in (0, T), \quad (2c)$$

inhomogeneous Dirichlet-Neumann mixed boundary conditions

$$q(t, 0) = 0 \quad \text{f.a.a. } t \in (0, T), \quad \mu_3 \kappa_2(L) q_x(t, L) = u(t) \quad \text{f.a.a. } t \in (0, T) \quad (2d)$$

and initial conditions

$$y(0, x) = y_o(x) \quad \text{f.a.a. } x \in \Omega. \quad (2e)$$

In the following, we will fix some assumptions for (2) that are necessary for our existence results.

Assumption 1.

- 1) For given parameter bounds $\boldsymbol{\mu}_a = (\mu_{a,i})_{1 \leq i \leq 4}$ and $\boldsymbol{\mu}_b = (\mu_{b,i})_{1 \leq i \leq 4}$ satisfying $0 < \boldsymbol{\mu}_a \leq \boldsymbol{\mu}_b$ in $\mathcal{P} = \mathbb{R}^4$ an admissible parameter vector $\boldsymbol{\mu} = (\mu_i)_{1 \leq i \leq 4}$ lies in the nonempty, compact and convex set $\mathcal{P}_{\text{ad}} = \{\boldsymbol{\mu} \in \mathcal{P} : \boldsymbol{\mu}_a \leq \boldsymbol{\mu} \leq \boldsymbol{\mu}_b \text{ in } \mathcal{P}\} \subset \mathcal{P}$. Here, ' \leq ' is understood component-wise.
- 2) The initial condition y_o belongs to $H^1(\Omega)$ and is positive on $\overline{\Omega}$, namely $y_o(x) \geq y_a$ for all $x \in \overline{\Omega}$ and a positive constant y_a .
- 3) For $\mathcal{U} := L^2(0, T)$ the set of admissible inputs is $\mathcal{U}_{\text{ad}} := \{u \in \mathcal{U} : u_a(t) \leq u(t) \leq u_b(t) \text{ f.a.a. } t \in [0, T]\}$ with $u_a, u_b \in L^\infty(0, T)$ satisfying $u_a \leq u_b$ a.e. in $[0, T]$. In particular, $\mathcal{U}_{\text{ad}} \subset L^\infty(0, T)$ holds, and we have $\|u\|_{L^\infty(0, T)} \leq c_{\mathcal{U}}$ for all $u \in \mathcal{U}$ with $c_{\mathcal{U}} = \max\{\|u_a\|_{L^\infty(0, T)}, \|u_b\|_{L^\infty(0, T)}\}$.
- 4) The functions κ_1, κ_2 belong to $C^{0,1}(\overline{\Omega})$ with $\kappa_1(x) \geq \kappa_a$ and $\kappa_2(x) \geq \kappa_a$ for all $x \in \overline{\Omega}$ and a positive constant κ_a .
- 5) The non-linearity is defined as $f(y, q) := \sqrt{y} \sinh(q)$ for $y \in \mathbb{R}_{\geq}$ and $q \in \mathbb{R}$.

Remark 2.1.

- 1) Recall that $H^1(\Omega) \hookrightarrow C(\overline{\Omega})$ holds (cf. [13]). Thus, Assumption 1-2) implies $y_o \in C(\overline{\Omega})$.
- 2) Note that f is not differentiable at $y = 0$. In our application, the state y stands for the concentration of lithium-ions in a battery cell. Thus, the situation $y = y(t, x) \leq 0$ does not have any physical meaning. This non-negativity of y is needed to evaluate $f(y, q)$. \diamond

Let $H := L^2(\Omega)$ and $V := H^1(\Omega)$ endowed with the inner products

$$\langle \varphi, \phi \rangle_H = \int_{\Omega} \varphi(x) \phi(x) \, dx \quad \text{for } \varphi, \phi \in H, \quad \langle \varphi, \phi \rangle_V = \int_{\Omega} \varphi(x) \phi(x) + \varphi'(x) \phi'(x) \, dx \quad \text{for } \varphi, \phi \in V,$$

respectively, and the associated induced norms $\|\cdot\|_H = \langle \cdot, \cdot \rangle_H^{1/2}$, $\|\cdot\|_V = \langle \cdot, \cdot \rangle_V^{1/2}$. We define the Hilbert space

$$V_o := \{\varphi \in V \mid \varphi(0) = 0\}$$

supplied by the inner product

$$\langle \varphi, \phi \rangle_{V_o} := \int_{\Omega} \varphi'(x) \phi'(x) \, dx \quad \text{for } \varphi, \phi \in V_o.$$

Furthermore, let $C_o(\overline{\Omega}) = \{\varphi \in C(\overline{\Omega}) : \varphi(0) = 0\}$ supplied with the $C(\overline{\Omega})$ -norm, i.e., $\|\varphi\|_{C(\overline{\Omega})} = \max_{x \in \overline{\Omega}} |\varphi(x)|$. Since $V \hookrightarrow C(\overline{\Omega})$ holds, there exists an embedding constant $c_e > 0$ (only dependent on the interval Ω) satisfying

$$\|\varphi\|_{C(\overline{\Omega})} \leq c_e \|\varphi\|_V \quad \text{for all } \varphi \in V \quad (3)$$

with $\|\varphi\|_{C(\overline{\Omega})} = \max_{x \in \overline{\Omega}} |\varphi(x)|$. Furthermore, Poincaré's inequality holds on the space V_\circ (see [38, Theorem 7.91]): there exists a constant $c_P > 0$ such that

$$\|\varphi\|_H \leq c_P \|\varphi\|_{V_\circ} \quad \text{for all } \varphi \in V_\circ. \quad (4)$$

From (3) and (4) we infer that

$$\|\varphi\|_{C(\overline{\Omega})}^2 \leq c_e^2 \|\varphi\|_V^2 = c_e^2 \left(\|\varphi\|_H^2 + \|\varphi\|_{V_\circ}^2 \right) \leq c_e^2 (c_P^2 + 1) \|\varphi\|_{V_\circ}^2.$$

Hence, for $c_{eP} = c_e(c_P^2 + 1)^{1/2} > 0$ it holds that

$$\|\varphi\|_{C(\overline{\Omega})} \leq c_{eP} \|\varphi\|_{V_\circ} \quad \text{for all } \varphi \in V_\circ. \quad (5)$$

Next, we define the solution spaces

$$\mathcal{Y}^T := W(0, T; V, V') \cap C(\overline{Q}_T) \quad \text{and} \quad \mathcal{Q}^T := L^\infty(0, T; V_\circ)$$

endowed by their product topology, where $W(0, T; X, Y) := L^2(0, T; X) \cap H^1(0, T; Y)$; see, e.g., [10] for more details. Moreover, for the function $x \mapsto \varphi(t, x)$ f.a.a. $t \in [0, T]$ with $\varphi \in L^2(0, T; V)$, we frequently use the notation $\varphi(t)$.

Throughout we write ‘a.e.’ for ‘almost everywhere’. Now, the weak formulation of (2) is as follows: for $\mu \in \mathcal{P}_{\text{ad}}$ and $u \in \mathcal{U}_{\text{ad}}$ find a solution pair $z = (y, q) \in \mathcal{Y}^T \times \mathcal{Q}^T$ such that

$$\frac{d}{dt} \langle y(t), \varphi^y \rangle_H + a_\mu^1(y(t), \varphi^y) + \langle g_\mu^1[z(t)], \varphi^y \rangle_{V', V} = 0 \quad \text{for all } \varphi^y \in V \text{ and } t \in (0, T] \text{ a.e.,} \quad (6a)$$

$$y(0) = y_\circ \quad \text{in } H, \quad (6b)$$

$$a_\mu^2(q(t), \varphi^q) + \langle g_\mu^2[z(t)], \varphi^q \rangle_{V_\circ', V_\circ} = \langle b(t), \varphi^q \rangle_{V_\circ', V_\circ} \quad \text{for all } \varphi^q \in V_\circ \text{ and } t \in (0, T] \text{ a.e.,} \quad (6c)$$

where the bilinear forms are defined as

$$a_\mu^1(\varphi, \phi) := \mu_1 \int_\Omega \kappa_1(x) \varphi'(x) \phi'(x) dx =: \mu_1 \hat{a}^1(\varphi, \phi) \quad \text{for } \varphi, \phi \in V, \quad (7a)$$

$$a_\mu^2(\varphi, \phi) := \mu_3 \int_\Omega \kappa_2(x) \varphi'(x) \phi'(x) dx =: \mu_3 \hat{a}^2(\varphi, \phi) \quad \text{for } \varphi, \phi \in V_\circ. \quad (7b)$$

The non-linear operators are given by

$$\langle g_\mu^1[z(t)], \varphi \rangle_{V', V} := \mu_2 \int_\Omega (-f(y(t), q(t))) \varphi(x) dx =: \mu_2 \hat{g}^1(z(t), \varphi) \quad \text{for } \varphi \in V, \quad (8a)$$

$$\langle g_\mu^2[z(t)], \varphi \rangle_{V_\circ', V_\circ} := \mu_4 \int_\Omega f(y(t), q(t)) \varphi(x) dx =: \mu_4 \hat{g}^2(z(t), \varphi) \quad \text{for } \varphi \in V_\circ, \quad (8b)$$

Finally, the boundary condition appears in the linear operator

$$\langle b(t), \varphi \rangle_{V_\circ', V_\circ} = u(t) \varphi(L) \quad \text{for } \varphi \in V_\circ \text{ and } t \in (0, T] \text{ a.e.}$$

2.2. Well-posedness of the state equation locally in time

Suppose that $y \in \mathcal{Y}^T$ with $y > 0$ in Q_T is given. For every $u \in \mathcal{U}_{\text{ad}}$ and f.a.a. $t \in [0, T]$ we consider the non-linear elliptic problem

$$-\mu_3 (\kappa_2 q_x(t))_x + \mu_4 f(y(t), q(t)) = 0 \text{ a.e. in } \Omega, \quad q(t, 0) = 0, \quad \mu_3 \kappa_2(L) q_x(t, L) = u(t). \quad (\mathbf{E})$$

A weak solution of **(E)** satisfies f.a.a. $t \in [0, T]$

$$\mu_3 \int_{\Omega} \kappa_2(x) q_x(t, x) \varphi'(x) dx + \mu_4 \int_{\Omega} f(y(t, x), q(t, x)) \varphi(x) dx = u(t) \varphi(L) \quad \text{for all } \varphi \in V_{\circ}. \quad (\mathbf{E}_w)$$

To prove the existence of a solution to **(E_w)** we make use of the Leray-Schauder fixed point theorem (cf., e.g. [14, p. 189]). For that purpose, the following hypothesis is needed.

Assumption 2. For a given $M > 1$ let y belong to the non-empty, closed, bounded, convex set \mathfrak{Y}_M^T defined as

$$\mathfrak{Y}_M^T := \left\{ y \in C(\overline{Q}_T) : \frac{1}{M} \leq y(t, x) \leq M \text{ for all } (t, x) \in \overline{Q}_T \right\}. \quad (9)$$

The following result is proved in Appendix A.1.

Theorem 2.2. *Let Assumptions 1 and 2 hold. Then, for every $u \in \mathcal{U}_{\text{ad}}$ there exists a unique solution $q \in \mathcal{Q}^T$ of **(E_w)** and a constant $c(M) > 0$ (independent of q or u but dependent on M) such that*

$$\|q(t)\|_{C(\overline{\Omega})} \leq c_{\text{eP}} \|q(t)\|_{V_{\circ}} \leq c(M) |u(t)| \leq c(M) c_{\mathcal{U}} \quad \text{for } t \in [0, T] \text{ a.e.}, \quad (10)$$

where the constant c_{eP} has already been introduced in (5).

In the following, we show the existence of the weak solution for the coupled system (1). The proof is based on the Schauder fixed point theorem and is given in Section A.2 of the appendix.

Theorem 2.3. *Let Assumptions 1 and 2 hold and the constant M in Assumption 2 be chosen as*

$$M = 2 \|y_{\circ}\|_{C(\overline{\Omega})} + \frac{2}{y_{\text{a}}}. \quad (11)$$

Then, there exists a finite time $T_{\circ} = T_{\circ}(M) \in (0, T]$ such that (2) admits a unique solution pair $z = (y, q) \in \mathfrak{Y}_M^{T_{\circ}} \times \mathcal{Q}^{T_{\circ}}$.

Remark 2.4. Note that, due to (11) we can see that $y_{\circ} \leq M/2$ and $y_{\circ} \geq y_{\text{a}} \geq 2/M$ for all $x \in \overline{\Omega}$. \diamond

3. THE DISCRETIZATION

Problem (6) has to be discretized for its numerical solution. First, we introduce a standard Galerkin approximation, which leads to a high-dimensional non-linear system of ordinary differential equations. Then, we formulate a reduced-order discretization.

3.1. The full-order discretization

The discretization of (6) is done in two steps. Suppose that $\{\varphi_i\}_{i=0}^n \subset V$ are linearly independent and that $\{\varphi_i\}_{i=1}^n \subset V_{\circ}$ holds. We define the finite-dimensional subspaces $V^h = \text{span}\{\varphi_0, \dots, \varphi_n\} \subset V$ and $V_{\circ}^h = \text{span}\{\varphi_1, \dots, \varphi_n\} \subset V_{\circ}$. Then, by Galerkin projection of equations (6) onto V^h and V_{\circ}^h , our goal is to find $z^h = (y^h, q^h) \in H^1(0, T; V^h) \times L^{\infty}(0, T; V_{\circ}^h)$ solving

$$\frac{d}{dt} \langle y^h(t), \varphi^y \rangle_H + a_{\mu}^1(y^h(t), \varphi^y) + \langle g_{\mu}^1[z^h(t)], \varphi^y \rangle_{V', V} = 0 \quad \text{for all } \varphi^y \in V^h \text{ and } t \in (0, T] \text{ a.e.}, \quad (12a)$$

$$\langle y^h(0) - y_{\circ}^h, \varphi^y \rangle_H = 0 \quad \text{for all } \varphi^y \in V^h, \quad (12b)$$

$$a_{\mu}^2(q^h(t), \varphi^q) + \langle g_{\mu}^2[z^h(t)], \varphi^q \rangle_{V', V_{\circ}} - \langle b(t), \varphi^q \rangle_{V_{\circ}', V_{\circ}} = 0 \quad \text{for all } \varphi^q \in V_{\circ}^h \text{ and } t \in [0, T] \text{ a.e.}, \quad (12c)$$

where y_\circ^h is a projection of y_\circ on V^h given as

$$y_\circ^h = \operatorname{argmin} \{ \|y_\circ - \varphi^h\|_H \mid \varphi^h \in V^h \}.$$

Note that

$$y^h(t) = \sum_{i=0}^n y_i(t) \varphi_i, \quad q^h(t) = \sum_{i=1}^n q_i(t) \varphi_i \quad \text{for } t \in [0, T]$$

so that (12) reduces into finding the coefficient vectors $y(t) = (y(t))_{0 \leq i \leq n}$ and $q(t) = (q(t))_{1 \leq i \leq n}$ solving the differential algebraic system

$$M_y \dot{y}(t) + \mu_1 A_1 y(t) - \mu_2 M_y f_y(y(t), q(t)) = 0 \quad t \in (0, T] \text{ a.e.}, \quad (13a)$$

$$M_y y(0) = y_\circ, \quad (13b)$$

$$\mu_3 A_2 q(t) + \mu_4 M_q f_q(y(t), q(t)) + b(t) = 0 \quad t \in [0, T] \text{ a.e.} \quad (13c)$$

for

$$\begin{aligned} M_y &= ((\langle \varphi_j, \varphi_i \rangle_H)) \in \mathbb{R}^{(n+1) \times (n+1)}, & A_1 &= ((\hat{a}^1(\varphi_j, \varphi_i))) \in \mathbb{R}^{(n+1) \times (n+1)} & \text{for } i, j = 0, \dots, n \\ y_\circ &= (\langle y_\circ, \varphi_i \rangle_H) \in \mathbb{R}^{n+1} & & & \text{for } i = 0, \dots, n, \\ M_q &= ((\langle \varphi_j, \varphi_i \rangle_H)) \in \mathbb{R}^{n \times n}, & A_2 &= ((\hat{a}^2(\varphi_j, \varphi_i))) \in \mathbb{R}^{n \times n} & \text{for } i, j = 1, \dots, n, \\ b(t) &= (\langle b(t), \varphi_i \rangle_{V_\circ', V_\circ}) \in \mathbb{R}^n & & & \text{for } i = 1, \dots, n. \end{aligned}$$

Moreover, $f_y(y(t), q(t)) \in \mathbb{R}^{n+1}$ (resp. $f_q(y(t), q(t)) \in \mathbb{R}^n$) is the coefficient vector satisfying

$$f(y^h(t, x), q^h(t, x)) \approx \left\{ \begin{array}{l} \sum_{j=0}^n f_{y,j}(y(t), q(t)) \varphi_j(x) \quad \text{in (13a),} \\ \sum_{j=1}^n f_{q,j}(y(t), q(t)) \varphi_j(x) \quad \text{in (13c)} \end{array} \right\} \quad \text{for } x \in \Omega \text{ and } t \in [0, T] \text{ a.e.}$$

Note that none of the matrices depend on μ due to the affine dependence of the parameters as in (7) and (8).

For solving (13) we apply the implicit Euler method for the time integration (cf., e.g., [35]) on an equidistant time grid $t_k = (k-1)\Delta t$, $k = 1, \dots, K$ and $\Delta t = T/(K-1)$. Then, the problem is to find $\{y^k\}_{k=1}^K \subset \mathbb{R}^{n+1}$ and $\{q^k\}_{k=1}^K \subset \mathbb{R}^n$ solving

$$\begin{aligned} M_y (y^k - y^{k-1}) + \mu_1 \Delta t A_1 y^k - \mu_2 \Delta t M_y f_y(y^k, q^k) &= 0 \quad \text{for } k = 2, \dots, K, \\ M_y y^1 &= y_\circ, \\ \mu_3 A_2 q^k + \mu_4 M_q f_q(y^k, q^k) + b^k &= 0 \quad \text{for } k = 1, \dots, K. \end{aligned} \quad (14)$$

These solutions are approximations of the FE solutions of (12) at each time step, namely

$$y^h(t_k) \approx \sum_{i=0}^n y_i^k \varphi_i \quad \text{and} \quad q^h(t_k) \approx \sum_{i=1}^n q_i^k \varphi_i \quad \text{for } k = 1, \dots, K.$$

Finally, to solve this non-linear system, we use Newton's method at each time step k , by defining the non-linear function

$$F_\mu(y^k, q^k) = \begin{pmatrix} (M_y + \mu_1 \Delta t A_1) y^k - M_y y^{k-1} - \mu_2 \Delta t M_y f(y^k, q^k) \\ \mu_3 A_2 q^k + \mu_4 M_q f(y^k, q^k) + b^k \end{pmatrix} \in \mathbb{R}^{2n+1}.$$

Then, the algorithm to evaluate the state variables given parameter μ is as follows:

- Evaluate y^1 by projecting the initial value.
- Compute q^1 solving the decoupled elliptic PDE given y^1 to get a consistent initial condition for the state q .
- For $k = 2, \dots, K$ find the root of the non-linear equation $F_\mu(y^k, q^k) = 0$.

3.2. The reduced-order discretization

In order to speed-up calculations, we construct reduced-order spaces $V^\ell \subset V^h$ and $V_o^\ell \subset V_o^h$, of dimensions respectively $\ell_y \ll n$ and $\ell_q \ll n$, and a set of basis for each space, $\{\psi_1^y, \dots, \psi_{\ell_y}^y\} \subset V^\ell$ and $\{\psi_1^q, \dots, \psi_{\ell_q}^q\} \subset V_o^\ell$. These spaces are evaluated by utilizing the proper orthogonal decomposition (POD) method (cf., e.g., [25]). Furthermore, $\Psi_y \in \mathbb{R}^{(n+1) \times \ell_y}$ is the matrix of coordinates of the basis $\{\psi_i^y\}_{i=1}^{\ell_y}$ with respect to the basis $\{\varphi_i\}_{i=0}^n$ of V^h , and similarly $\Psi_q \in \mathbb{R}^{n \times \ell_q}$ is the matrix of coordinates of the basis $\{\psi_i^q\}_{i=1}^{\ell_q}$ with respect to the basis $\{\varphi_i\}_{i=1}^n$ of V_o^h . Namely,

$$\psi_j^y = \sum_{i=0}^n (\Psi_y)_{ij} \varphi_i \text{ for } j = 1, \dots, \ell_y \quad \text{and} \quad \psi_j^q = \sum_{i=1}^n (\Psi_q)_{ij} \varphi_i \text{ for } j = 1, \dots, \ell_q.$$

As a first step we project all matrices on the reduced spaces so that a reduced-order approximation of (14) reads as follows: find $\{\hat{y}^k\}_{k=1}^K \subset \mathbb{R}^{\ell_y}$ and $\{\hat{q}^k\}_{k=1}^K \subset \mathbb{R}^{\ell_q}$ such that

$$\begin{aligned} (M_y^\ell + \mu_1 \Delta t A_1^\ell) \hat{y}^k - M_y^\ell \hat{y}^{k-1} - \mu_2 \Delta t \Psi_y^\top M_y f_y(\Psi_y \hat{y}^k, \Psi_q \hat{q}^k) &= 0 \quad \text{for } k = 2, \dots, K, \\ M_y^\ell \hat{y}^1 &= y_o^\ell, \\ \mu_3 A_2^\ell \hat{q}^k + \mu_4 \Psi_q^\top M_q f_q(\Psi_y \hat{y}^k, \Psi_q \hat{q}^k) + b^{k,\ell} &= 0 \quad \text{for } k = 1, \dots, K \end{aligned} \tag{15}$$

with $M_y^\ell = \Psi_y^\top M_y \Psi_y$, $A_1^\ell = \Psi_y^\top A_1 \Psi_y$, $A_2^\ell = \Psi_q^\top A_2 \Psi_q$, $b^{k,\ell} = \Psi_q^\top b^k$ for $k = 1, \dots, K$, and $y_o^\ell = \Psi_y^\top y_o$.

System (15) still depends on dimension n through the evaluation of the non-linearities f_y and f_q . We can use the empirical interpolation method (EIM) or the discrete empirical interpolation method (DEIM) (cf., e.g., [6] and [8]) to make the evaluation of the system independent of n . In our case, we use DEIM where, in a nutshell, the vectors $f_y^k := f_y(\Psi_y \hat{y}^k, \Psi_q \hat{q}^k)$ and $f_q^k := f_q(\Psi_y \hat{y}^k, \Psi_q \hat{q}^k)$ for $k = 1, \dots, K$ are projected onto a smaller space of dimension $\ell_f \ll n$. For the q-system this is done by finding matrices $\Psi_f \in \mathbb{R}^{n \times \ell_f}$, and $P \in \mathbb{R}^{n \times \ell_f}$ such that

$$f^k \approx \Psi_f (P^\top \Psi_f)^{-1} P^\top f^k,$$

where the matrix Ψ_f is given by the POD method using the snapshots f^k for $k = 1, \dots, K$. The matrix P is, on the other hand, composed only by zeros and ones such that $P^\top v \in \mathbb{R}^{\ell_f}$ contains only selected rows of $v \in \mathbb{R}^n$. For more information, see [8].

Remark 3.1. For the y-system (of dimension $n + 1$) we set

$$\tilde{\Psi}_f = \begin{bmatrix} 0 \\ \Psi_f \end{bmatrix} \in \mathbb{R}^{(n+1) \times \ell_f}, \quad \tilde{P} = \begin{bmatrix} 0 \\ P \end{bmatrix} \in \mathbb{R}^{(n+1) \times \ell_f},$$

and get $\tilde{f}^k \approx \tilde{\Psi}_f (\tilde{P}^\top \tilde{\Psi}_f)^{-1} \tilde{P}^\top \tilde{f}^k \in \mathbb{R}^{n+1}$. ◇

Since the evaluation of f^k is done component-wise, we can write

$$P^\top f^k = P^\top f(\Psi_y \hat{y}^k, \Psi_q \hat{q}^k) = f(\tilde{P}^\top \Psi_y \hat{y}^k, P^\top \Psi_q \hat{q}^k) =: f(\hat{\Psi}_y \hat{y}^k, \hat{\Psi}_q \hat{q}^k)$$

for $\hat{\Psi}_y = \tilde{P}^\top \Psi_y \in \mathbb{R}^{\ell_f \times \ell_y}$ and $\hat{\Psi}_q = P^\top \Psi_q \in \mathbb{R}^{\ell_f \times \ell_q}$. Then, for

$$G_y = \Psi_y^\top M_y \tilde{\Psi}_f (\tilde{P}^\top \tilde{\Psi}_f)^{-1} \in \mathbb{R}^{\ell_y \times \ell_f} \quad \text{and} \quad G_q = \Psi_q^\top M_q \Psi_f (P^\top \Psi_f)^{-1} \in \mathbb{R}^{\ell_q \times \ell_f}$$

system (15) is approximated by

$$\begin{aligned} (M_y^\ell + \mu_1 \Delta t A_1^\ell) \hat{y}^k - M_y^\ell \hat{y}^{k-1} - \mu_2 \Delta t G_y f(\hat{\Psi}_y \hat{y}^k, \hat{\Psi}_q \hat{q}^k) &= 0 \quad \text{for } k = 2, \dots, K, \\ M_y^\ell \hat{y}^1 &= y_o^\ell, \\ \mu_3 A_2^\ell \hat{q}^k + \mu_4 G_q f(\hat{\Psi}_y \hat{y}^k, \hat{\Psi}_q \hat{q}^k) + b^{k,\ell} &= 0 \quad \text{for } k = 1, \dots, K, \end{aligned} \quad (16)$$

which is finally independent of n . In the following, we call system (16) reduced-order (RO) model. The RO solutions $\{\hat{y}^k\}_{k=1}^K \subset \mathbb{R}^{\ell_y}$ and $\{\hat{q}^k\}_{k=1}^K \subset \mathbb{R}^{\ell_q}$ are interpreted as a reduced-order approximations for $\{y^k\}_{k=1}^K \subset \mathbb{R}^{n+1}$ and $\{q^k\}_{k=1}^K \subset \mathbb{R}^n$, namely

$$y^k \approx y^{k,\ell} := \Psi_y \hat{y}^k \quad \text{and} \quad q^k \approx q^{k,\ell} := \Psi_q \hat{q}^k.$$

4. HIERARCHICAL A-POSTERIORI ERROR FOR THE STATE EQUATION

The accuracy of the reduced-order solution is controlled by hierarchical error estimates. Here we extend the approach in [21] to the time-dependent and non-linear coupled system (2).

4.1. The error estimator

From now on, we add the dependence on the parameter $\boldsymbol{\mu}$. Namely, $\{y^k(\boldsymbol{\mu})\}_{k=1}^K$ and $\{q^k(\boldsymbol{\mu})\}_{k=1}^K$ are the FE solutions (solving (14)), while $\{\hat{y}^k(\boldsymbol{\mu})\}_{k=1}^K$ and $\{\hat{q}^k(\boldsymbol{\mu})\}_{k=1}^K$ are the ROM solutions (solving problem (16)) with parameter $\boldsymbol{\mu} \in \mathcal{P}_{\text{ad}}$.

A-posteriori estimates are needed to control the error of the reduced-order approximation without knowing the full-order solution (see, e.g., [3, 19, 20]). These estimates give us upper bounds for the error of the differences $y^k(\boldsymbol{\mu}) - y^{k,\ell}(\boldsymbol{\mu})$ and $q^k(\boldsymbol{\mu}) - q^{k,\ell}(\boldsymbol{\mu})$ without actually evaluating the FE solutions (whose evaluation can lead up to long computation time). While it is possible to use residual-based norms (as in the case of the error estimate in [19]), in the non-linear framework this is not online efficient, since the evaluation of the coupling term needs to be done in the full FE dimensions n .

In this section we will utilize hierarchical error estimators which are well-known, e.g., for adaptive finite elements; cf. [5, 9, 11], for instance. The idea is to use the difference between two approximations with different orders to estimate the RB error. Here we define (approximated) hierarchical error estimators for the RB method applying the ideas in [21]. Given RB spaces V^ℓ and V_o^ℓ , with respective reduced bases associated with the matrices Ψ_y^ℓ and Ψ_q^ℓ , we define the RB errors as

$$E_y^\ell(\boldsymbol{\mu}) := \left(\sum_{k=1}^K \alpha_k \|y^k(\boldsymbol{\mu}) - y^{k,\ell}(\boldsymbol{\mu})\|_{S_y}^2 \right)^{1/2} \quad \text{and} \quad E_q^\ell(\boldsymbol{\mu}) := \left(\sum_{k=1}^K \alpha_k \|q^k(\boldsymbol{\mu}) - q^{k,\ell}(\boldsymbol{\mu})\|_{S_q}^2 \right)^{1/2},$$

where the α_k 's are trapezoidal weights, $S_y = ((\langle \varphi_j, \varphi_i \rangle_V))_{0 \leq i, j \leq n}$ and $S_q = ((\langle \varphi_j, \varphi_i \rangle_{V_o}))_{1 \leq i, j \leq n}$ are positive definite, symmetric weighting matrices. These errors approximate the errors $y^h - y^\ell$ and $q^h - q^\ell$ in the $L^2(0, T; V)$ - and $L^2(0, T; V_o)$ -norms, respectively. If we had another couple of RB spaces, V^m and V_o^m with $\ell_y < m_y \ll n$ and $\ell_q < m_q \ll n$ such that $E_y^m(\boldsymbol{\mu}) \leq \varepsilon$ and $E_q^m(\boldsymbol{\mu}) \leq \varepsilon$, then using the triangular inequality we get

$$\begin{aligned} E_y^\ell(\boldsymbol{\mu})^2 &= \sum_{k=1}^K \alpha_k \|y^k(\boldsymbol{\mu}) - y^{k,\ell}(\boldsymbol{\mu})\|_{S_y}^2 \leq \sum_{k=1}^K \alpha_k \|y^k(\boldsymbol{\mu}) - y^{k,m}(\boldsymbol{\mu})\|_{S_y}^2 + \sum_{k=1}^K \alpha_k \|y^{k,m}(\boldsymbol{\mu}) - y^{k,\ell}(\boldsymbol{\mu})\|_{S_y}^2 \\ &\leq \varepsilon^2 + \Delta_y^{\ell,m}(\boldsymbol{\mu})^2 \end{aligned}$$

and, similarly, $E_q^\ell(\boldsymbol{\mu})^2 \leq \varepsilon^2 + \Delta_q^{\ell,m}(\boldsymbol{\mu})^2$ with the computable quantities

$$\Delta_y^{\ell,m}(\boldsymbol{\mu})^2 := \sum_{k=1}^K \alpha_k \|y^{k,m}(\boldsymbol{\mu}) - y^{k,\ell}(\boldsymbol{\mu})\|_{S_y}^2 \quad \text{and} \quad \Delta_q^{\ell,m}(\boldsymbol{\mu})^2 := \sum_{k=1}^K \alpha_k \|q^{k,m}(\boldsymbol{\mu}) - q^{k,\ell}(\boldsymbol{\mu})\|_{S_q}^2.$$

These estimates are online-efficient (i.e., their evaluation does not depend on the FE dimension n), since

$$\begin{aligned} \Delta_y^{\ell,m}(\boldsymbol{\mu})^2 &= \sum_{k=1}^K \alpha_k (\hat{y}^{k,m}(\boldsymbol{\mu})^\top S_y^{m,m} \hat{y}^{k,m}(\boldsymbol{\mu}) - 2\hat{y}^{k,m}(\boldsymbol{\mu})^\top S_y^{m,\ell} \hat{y}^{k,\ell}(\boldsymbol{\mu}) + y^{k,\ell}(\boldsymbol{\mu})^\top S_y^{\ell,\ell} \hat{y}^{k,\ell}(\boldsymbol{\mu})), \\ \Delta_q^{\ell,m}(\boldsymbol{\mu})^2 &= \sum_{k=1}^K \alpha_k (\hat{q}^{k,m}(\boldsymbol{\mu})^\top S_q^{m,m} \hat{q}^{k,m}(\boldsymbol{\mu}) - 2\hat{q}^{k,m}(\boldsymbol{\mu})^\top S_q^{m,\ell} \hat{q}^{k,\ell}(\boldsymbol{\mu}) + q^{k,\ell}(\boldsymbol{\mu})^\top S_q^{\ell,\ell} \hat{q}^{k,\ell}(\boldsymbol{\mu})), \end{aligned}$$

where $\{\hat{y}^{k,\ell}(\boldsymbol{\mu}), \hat{q}^{k,\ell}(\boldsymbol{\mu})\}_{k=1}^K$ (resp. $\{\hat{y}^{k,m}(\boldsymbol{\mu}), \hat{q}^{k,m}(\boldsymbol{\mu})\}_{k=1}^K$) are the solution of (16) in dimensions ℓ_y and ℓ_q (resp. m_y and m_q), $S_y^{m,m} = \Psi_y^{m,\top} S_y \Psi_y^m \in \mathbb{R}^{m_y \times m_y}$, $S_y^{m,\ell} = \Psi_y^{m,\top} S_y \Psi_y^\ell \in \mathbb{R}^{m_y \times \ell_y}$, $S_y^{\ell,\ell} = \Psi_y^{\ell,\top} S_y \Psi_y^\ell \in \mathbb{R}^{\ell_y \times \ell_y}$, and the matrices $S_q^{m,m}$, $S_q^{m,\ell}$, $S_q^{\ell,\ell}$ are defined similarly.

To analyze the hierarchical error estimates it is useful to set $V^\ell \subset V^m$ and $V_o^\ell \subset V_o^m$ and to assume the following *saturation property* on the bigger RB space V^m : there exist $\sigma_y, \sigma_q \in (0, 1)$ such that

$$E_y^m(\boldsymbol{\mu})^2 \leq \sigma_y E_y^\ell(\boldsymbol{\mu})^2 \quad \text{and} \quad E_q^m(\boldsymbol{\mu})^2 \leq \sigma_q E_q^\ell(\boldsymbol{\mu})^2 \quad \text{for all } \boldsymbol{\mu} \in \mathcal{P}_{\text{ad}}. \quad (17)$$

This is a natural assumption since one expects the RB error to decrease with the increase of the RB dimension, but this condition will be enforced during the construction of the spaces V^m and V_o^m .

Proposition 4.1. *If (17) holds, then for all $\boldsymbol{\mu} \in \mathcal{P}_{\text{ad}}$*

$$\frac{\Delta_y^{\ell,m}(\boldsymbol{\mu})^2}{1 + \sigma_y} \leq E_y^\ell(\boldsymbol{\mu})^2 = \sum_{k=1}^K \alpha_k \|y^k(\boldsymbol{\mu}) - y^{k,\ell}(\boldsymbol{\mu})\|_{S_y}^2 \leq \frac{\Delta_y^{\ell,m}(\boldsymbol{\mu})^2}{1 - \sigma_y}, \quad (18a)$$

$$\frac{\Delta_q^{\ell,m}(\boldsymbol{\mu})^2}{1 + \sigma_q} \leq E_q^\ell(\boldsymbol{\mu})^2 = \sum_{k=1}^K \alpha_k \|q^k(\boldsymbol{\mu}) - q^{k,\ell}(\boldsymbol{\mu})\|_{S_q}^2 \leq \frac{\Delta_q^{\ell,m}(\boldsymbol{\mu})^2}{1 - \sigma_q}. \quad (18b)$$

Proof. We only prove (18a). The proof of (18b) is similar. If $\|y^k(\boldsymbol{\mu}) - y^{k,\ell}(\boldsymbol{\mu})\|_{S_y} = 0$ for $k = 1, \dots, K$, then $\|y^k(\boldsymbol{\mu}) - y^{k,m}(\boldsymbol{\mu})\|_{S_y} = 0$ for $k = 1, \dots, K$ as well. Thus we get $\Delta_y^{\ell,m}(\boldsymbol{\mu}) = 0$ so that (18a) follows. Otherwise, using the reverse triangle inequality and (17) we get

$$\begin{aligned} \frac{\sum_{k=1}^K \alpha_k \|y^{k,\ell}(\boldsymbol{\mu}) - y^{k,m}(\boldsymbol{\mu})\|_{S_y}^2}{\sum_{k=1}^K \alpha_k \|y^k(\boldsymbol{\mu}) - y^{k,\ell}(\boldsymbol{\mu})\|_{S_y}^2} &\geq \frac{\sum_{k=1}^K \alpha_k \|y^k(\boldsymbol{\mu}) - y^{k,\ell}(\boldsymbol{\mu})\|_{S_y}^2 - \sum_{k=1}^K \alpha_k \|y^k(\boldsymbol{\mu}) - y^{k,m}(\boldsymbol{\mu})\|_{S_y}^2}{\sum_{k=1}^K \alpha_k \|y^k(\boldsymbol{\mu}) - y^{k,\ell}(\boldsymbol{\mu})\|_{S_y}^2} \\ &\geq 1 - \frac{\sum_{k=1}^K \alpha_k \|y^k(\boldsymbol{\mu}) - y^{k,m}(\boldsymbol{\mu})\|_{S_y}^2}{\sum_{k=1}^K \alpha_k \|y^k(\boldsymbol{\mu}) - y^{k,\ell}(\boldsymbol{\mu})\|_{S_y}^2} = 1 - \frac{E_y^m(\boldsymbol{\mu})^2}{E_y^\ell(\boldsymbol{\mu})^2} \geq 1 - \sigma_y. \end{aligned}$$

On the other hand, using the triangle inequality and (17),

$$\begin{aligned} \frac{\sum_{k=1}^K \alpha_k \|y^{k,\ell}(\boldsymbol{\mu}) - y^{k,m}(\boldsymbol{\mu})\|_{S_y}^2}{\sum_{k=1}^K \alpha_k \|y^k(\boldsymbol{\mu}) - y^{k,\ell}(\boldsymbol{\mu})\|_{S_y}^2} &\leq \frac{\sum_{k=1}^K \alpha_k \|y^k(\boldsymbol{\mu}) - y^{k,\ell}(\boldsymbol{\mu})\|_{S_y}^2 + \sum_{k=1}^K \alpha_k \|y^k(\boldsymbol{\mu}) - y^{k,m}(\boldsymbol{\mu})\|_{S_y}^2}{\sum_{k=1}^K \alpha_k \|y^k(\boldsymbol{\mu}) - y^{k,\ell}(\boldsymbol{\mu})\|_{S_y}^2} \\ &\leq 1 + \frac{\sum_{k=1}^K \alpha_k \|y^k(\boldsymbol{\mu}) - y^{k,m}(\boldsymbol{\mu})\|_{S_y}^2}{\sum_{k=1}^K \alpha_k \|y^k(\boldsymbol{\mu}) - y^{k,\ell}(\boldsymbol{\mu})\|_{S_y}^2} = 1 + \frac{E_y^m(\boldsymbol{\mu})^2}{E_y^\ell(\boldsymbol{\mu})^2} \leq 1 + \sigma_y, \end{aligned}$$

which gives (18a). □

Next, we define the hierarchical error estimators in $\boldsymbol{\mu} \in \mathcal{P}_{\text{ad}}$ as

$$\Delta_y^\ell(\boldsymbol{\mu}) = \Delta_y^\ell(\boldsymbol{\mu}; m, \sigma_y) = \frac{\Delta_y^{\ell,m}(\boldsymbol{\mu})}{\sqrt{1 - \sigma_y}} \quad \text{and} \quad \Delta_q^\ell(\boldsymbol{\mu}) = \Delta_q^\ell(\boldsymbol{\mu}; m, \sigma_q) = \frac{\Delta_q^{\ell,m}(\boldsymbol{\mu})}{\sqrt{1 - \sigma_q}}. \quad (19)$$

Remark 4.2. The effectivities of the estimate in the parameter $\boldsymbol{\mu} \in \mathcal{P}_{\text{ad}}$ are defined as

$$\eta_y(\boldsymbol{\mu}) := \frac{\Delta_y^\ell(\boldsymbol{\mu})}{E_y^\ell(\boldsymbol{\mu})} \quad \text{and} \quad \eta_q(\boldsymbol{\mu}) := \frac{\Delta_q^\ell(\boldsymbol{\mu})}{E_q^\ell(\boldsymbol{\mu})}. \quad (20)$$

Then, we infer from (20), (18) and (19) that

$$1 \leq \eta_y(\boldsymbol{\mu}) \leq \bar{\eta}_y := \sqrt{\frac{1 + \sigma_y}{1 - \sigma_y}} \quad \text{and} \quad 1 \leq \eta_q(\boldsymbol{\mu}) \leq \bar{\eta}_q := \sqrt{\frac{1 + \sigma_q}{1 - \sigma_q}} \quad \text{for all } \boldsymbol{\mu} \in \mathcal{P}_{\text{ad}}. \quad (21)$$

Hence we observe that the closer σ_y (respectively σ_q) is to 0, the more accurate the estimate $\Delta_y^\ell(\boldsymbol{\mu})$ (resp. $\Delta_q^\ell(\boldsymbol{\mu})$) is for any $\boldsymbol{\mu} \in \mathcal{P}_{\text{ad}}$. ◇

There are two important choices to be made: the first is how to compute σ_y and σ_q , and the second is how to choose the RB spaces V^m and V_\circ^m . For the first issue, we compute approximations $\tilde{\sigma}_y$ and $\tilde{\sigma}_q$ on a training set, namely

$$\sigma_y \approx \tilde{\sigma}_y := \max_{\boldsymbol{\mu} \in \mathcal{P}_{\text{train}}} \frac{E_y^m(\boldsymbol{\mu})^2}{E_y^\ell(\boldsymbol{\mu})^2} \quad \text{and} \quad \sigma_q \approx \tilde{\sigma}_q := \max_{\boldsymbol{\mu} \in \mathcal{P}_{\text{train}}} \frac{E_q^m(\boldsymbol{\mu})^2}{E_q^\ell(\boldsymbol{\mu})^2}. \quad (22)$$

Let us observe that the computation of (22) can be done efficiently by parallelization.

Next, the second question is answered by defining V^m (resp. V_\circ^m) as an expansion of V^ℓ (resp. V_\circ^ℓ), namely $V^\ell \subset V^m$ and $V_\circ^\ell \subset V_\circ^m$. In particular, given V^ℓ and V_\circ^ℓ , we will find $\tilde{V}^m \perp V^\ell$ and $\tilde{V}_\circ^m \perp V_\circ^\ell$ and then define

$$V^m = V^\ell \oplus \tilde{V}^m \quad \text{and} \quad V_\circ^m = V_\circ^\ell \oplus \tilde{V}_\circ^m, \quad (23)$$

where \oplus is the direct sum (cf. e.g., [5]). The greedy algorithm for the evaluation of the RB spaces is shown in Algorithm 1. The input of the algorithm are the tolerance $\tau > 0$, an initial parameter $\boldsymbol{\mu} = (\mu_i)_{1 \leq i \leq 4} \in \mathcal{P}_{\text{ad}}$, a training set $\mathcal{P}_{\text{train}}$ and the maximum RB cardinality $L > 0$. The maximum number of bases elements is a safeguard in case the maximum error does not go under tolerance.

In line 2 the computation of the initial RB spaces is described. As a first step, we create RB spaces V^ℓ and V_\circ^ℓ using POD with the state variables' snapshots $\{y^k(\boldsymbol{\mu})\}_{k=1}^K$ and $\{q^k(\boldsymbol{\mu})\}_{k=1}^K$. Then, to define \tilde{V}^m and \tilde{V}_\circ^m we use the sensitivity variables (as suggested in [21]). In particular, we first evaluate the vectors $\{s_{y,i}^k(\boldsymbol{\mu}), s_{q,i}^k(\boldsymbol{\mu})\}_{k=1}^K$ for $i = 1, \dots, 4$, where $s_{y,i}^k(\boldsymbol{\mu})$ is the coordinate vector of FE approximation of the i -th sensitivity variable w.r.t. state variable y evaluated at t_k using parameter $\boldsymbol{\mu}$. Secondly, we orthogonalize the vectors $\{y^k(\boldsymbol{\mu}), s_{y,i}^k(\boldsymbol{\mu})\}_{k=1}^K$ (resp. $\{q^k(\boldsymbol{\mu}), s_{q,i}^k(\boldsymbol{\mu})\}_{k=1}^K$) for $i = 1, \dots, 4$ w.r.t. V^ℓ (resp. V_\circ^ℓ). Finally, we use POD on the two sets of vectors to evaluate \tilde{V}^m and \tilde{V}_\circ^m . Then, line 6 uses (23) to define the spaces V^m and V_\circ^m . We observe that by construction $V^\ell \perp \tilde{V}^m$ and $V_\circ^\ell \perp \tilde{V}_\circ^m$, though it is possible to orthogonalize the bases to enforce this condition numerically. Furthermore, we add that at first we choose $m_y = \ell_y + 2$ and $m_q = \ell_q + 2$, namely we construct the initial \tilde{V}^m and \tilde{V}_\circ^m of dimension 2.

Lines 7 and 21 evaluates $\tilde{\sigma}_y$ and $\tilde{\sigma}_q$. If $\tilde{\sigma}_y > 1$ or $\tilde{\sigma}_q > 1$ (as in line 4), it means that the saturation property is violated. This has so far not happened to us, confirming the expectation that a bigger RB space is a better approximation of the FE space for any $\boldsymbol{\mu} \in \mathcal{P}_{\text{ad}}$. But in case this condition is violated, our algorithm enriches the spaces \tilde{V}^m and \tilde{V}_\circ^m in the parameters where such condition was violated. Enriching here means evaluating

Algorithm 1 (Weak Greedy algorithm)

Require: $\tau > 0$, $\hat{\boldsymbol{\mu}} \in \mathcal{P}_{\text{ad}}$, $\mathcal{P}_{\text{train}} \subset \mathcal{P}_{\text{ad}}$, $L > 0$;

- 1: Create RB spaces V^ℓ , V_\circ^ℓ , \tilde{V}^m and \tilde{V}_\circ^m in $\hat{\boldsymbol{\mu}}$;
- 2: $V^m \leftarrow V^\ell \oplus \tilde{V}^m$ and $V_\circ^m \leftarrow V_\circ^\ell \oplus \tilde{V}_\circ^m$ as in (23);
- 3: Evaluate $\tilde{\sigma}_y$ and $\tilde{\sigma}_q$ as in (22);
- 4: **while** $\tilde{\sigma}_y \geq 1$ **or** $\tilde{\sigma}_q \geq 1$ **do**
- 5: Enrich \tilde{V}^m and/or \tilde{V}_\circ^m ;
- 6: Set $V^m \leftarrow V^\ell \oplus \tilde{V}^m$ and $V_\circ^m \leftarrow V_\circ^\ell \oplus \tilde{V}_\circ^m$;
- 7: Evaluate $\tilde{\sigma}_y$ and $\tilde{\sigma}_q$ as in (22);
- 8: **end while**
- 9: Evaluate $\hat{\boldsymbol{\mu}} = \arg \max_{\boldsymbol{\mu} \in \mathcal{P}_{\text{train}}} e^\ell(\boldsymbol{\mu}) := (\Delta_y^\ell(\boldsymbol{\mu}) + \Delta_q^\ell(\boldsymbol{\mu}))/2$ and $\hat{e} = e(\hat{\boldsymbol{\mu}})$;
- 10: **while** $\hat{e} > \tau$ **and** $\ell_y + \ell_q < L$ **do**
- 11: **if** $\Delta_y^\ell(\hat{\boldsymbol{\mu}}) > \tau$ **then**
- 12: Enrich V^ℓ in $\hat{\boldsymbol{\mu}}$;
- 13: **end if**
- 14: **if** $\Delta_q^\ell(\hat{\boldsymbol{\mu}}) > \tau$ **then**
- 15: Enrich V_\circ^ℓ in $\hat{\boldsymbol{\mu}}$;
- 16: **end if**
- 17: Set $V^m \leftarrow V^\ell \oplus \tilde{V}^m$ and $V_\circ^m \leftarrow V_\circ^\ell \oplus \tilde{V}_\circ^m$;
- 18: **while** $\tilde{\sigma}_y \geq 1$ **or** $\tilde{\sigma}_q \geq 1$ **do**
- 19: Enrich \tilde{V}^m and \tilde{V}_\circ^m ;
- 20: Set $V^m \leftarrow V^\ell \oplus \tilde{V}^m$ and $V_\circ^m \leftarrow V_\circ^\ell \oplus \tilde{V}_\circ^m$;
- 21: Evaluate $\tilde{\sigma}_y$ and $\tilde{\sigma}_q$ as in (22);
- 22: **end while**
- 23: Evaluate $\hat{\boldsymbol{\mu}} = \arg \max_{\boldsymbol{\mu} \in \mathcal{P}_{\text{train}}} e^\ell(\boldsymbol{\mu}) := (\Delta_y^\ell(\boldsymbol{\mu}) + \Delta_q^\ell(\boldsymbol{\mu}))/2$ and $\hat{e} = e(\hat{\boldsymbol{\mu}})$;
- 24: **end while**

FE vectors, orthogonalizing w.r.t. V^m or V_\circ^m , and then using POD to add some new bases to them. This procedure is then applied as long as the saturation property is violated.

Lines 9 and 23 evaluate the error measure we want to lower. If this error is higher than a certain tolerance, it means that either $\Delta_y^\ell(\hat{\boldsymbol{\mu}}) > \tau$ or $\Delta_q^\ell(\hat{\boldsymbol{\mu}}) > \tau$ (or, eventually, both). Then the enrichment is done by evaluating the states' snapshots, orthogonalizing them w.r.t. the bases we already have and then using POD to get new elements. We can then add as many elements such that $\Delta_y^\ell(\hat{\boldsymbol{\mu}}) \leq \tau$ and $\Delta_q^\ell(\hat{\boldsymbol{\mu}}) \leq \tau$.

We then check $\tilde{\sigma}_y$ and $\tilde{\sigma}_q$ again. Since V^ℓ and V_\circ^ℓ could have been enriched, we need to orthogonalize \tilde{V}^m and \tilde{V}_\circ^m with respect to them. It still holds that $V^\ell \subset V^m$ and $V_\circ^\ell \subset V_\circ^m$, but if the saturation property fails, we enforce it by enriching \tilde{V}^m or \tilde{V}_\circ^m .

4.2. Numerical experiments

Let us now set $\Omega = (0, 1)$ and $T = 1$, discretized with linear Lagrangian elements in space on 200 spatial nodes (so that $n = 201$) and the implicit Euler method for $K = 201$ time steps. We choose the diffusion functions $\kappa_1(x) \equiv \kappa_2(x) \equiv 1$, initial value $y_\circ(x) \equiv 5$ and parameter bounds as $\mu_{\text{a},i} = 1$ and $\mu_{\text{b},i} = 5$ for $i = 1, \dots, 4$. The set $\mathcal{P}_{\text{train}}$ is chosen as a uniform grid $5 \times 5 \times 5 \times 5$ on \mathcal{P}_{ad} , such that $\mathcal{P}_{\text{train}} = \{\boldsymbol{\mu} \in \mathbb{R}^4 \mid \mu_i \in \{1, 2, 3, 4, 5\} \text{ for } i = 1, 2, 3, 4\}$. Furthermore, we choose $\tau = 10^{-4}$ and $L = 50$.

We analyse the results of the greedy algorithm and the generated RB spaces using three different input functions, namely

$$u_1(t) \equiv 1, \quad u_2(t) = -\mathbf{1}_{[0,0.75)}(t) + \mathbf{1}_{[0.75,1]}(t), \quad u_3(t) = 0.5 \cdot \cos(10t) + 0.4 \cdot \sin(20t) \quad \text{for } t \in [0, T],$$

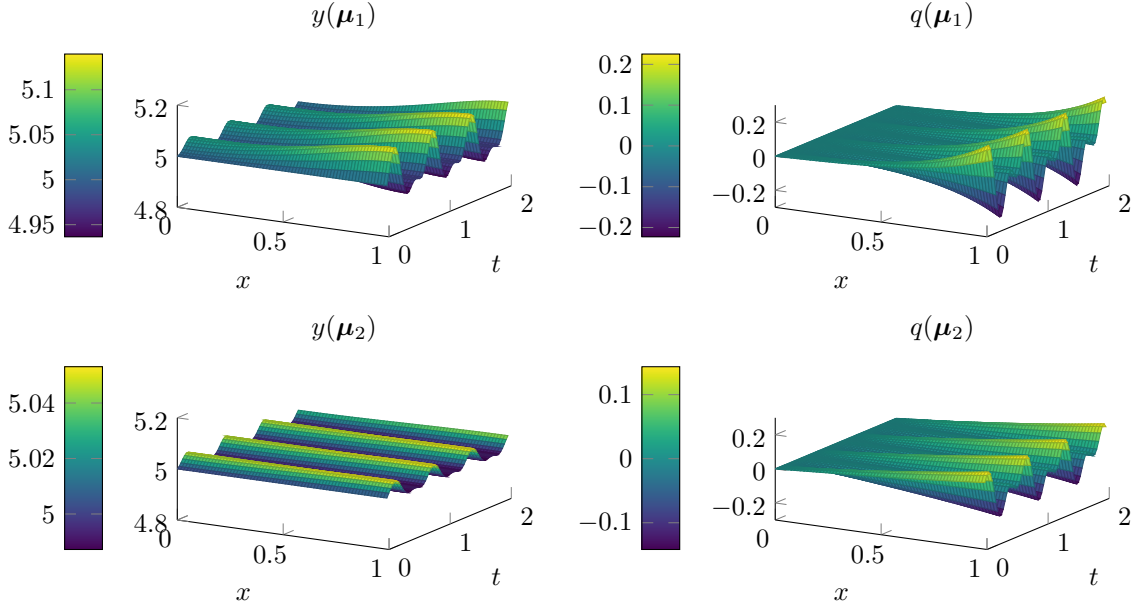


FIGURE 1. State variables for $\mu_1 = (1, 5, 1, 5)$ and $\mu_2 = (5, 3, 4, 2)$.

where $\mathbf{1}_I(t)$ is the indicator function of interval I . To give an idea of what state variables look like, we show in Figure 1 approximated FE states for input function u_3 .

We will compare the overall time of the Algorithm 1, the number of bases generated in all spaces, the approximated values $\tilde{\sigma}_y$ and $\tilde{\sigma}_q$ and the respective approximated efficiency, $\tilde{\eta}_y$ and $\tilde{\eta}_q$ given as (21); cf. Table 1. Furthermore, given a set $\mathcal{P}_{\text{test}}$ of 100 random parameters in \mathcal{P}_{ad} , we evaluate the average times of evaluating FE and RB states, maximum test errors

$$\hat{E}_y^\ell = \max_{\mu \in \mathcal{P}_{\text{test}}} E_y^\ell(\mu) \quad \text{and} \quad \hat{E}_q^\ell = \max_{\mu \in \mathcal{P}_{\text{test}}} E_q^\ell(\mu)$$

and maximum test efficiencies

$$\hat{\eta}_y = \max_{\mu \in \mathcal{P}_{\text{test}}} \eta_y(\mu) \quad \text{and} \quad \hat{\eta}_q = \max_{\mu \in \mathcal{P}_{\text{test}}} \eta_q(\mu),$$

where $\eta_y(\mu)$ and $\eta_q(\mu)$ are defined in (20).

The overall algorithm time does not change much with different inputs. The evaluation of \hat{e} in lines 9 and 23 does not take much CPU time. On the contrary, the evaluation of (22) takes necessarily more time, because the evaluation of $\tilde{\sigma}_y$ and $\tilde{\sigma}_q$ needs the evaluation of the FE solutions, while the evaluation of $e^\ell(\mu)$ does not. We can see that the bigger spaces V^m and V_o^m are in fact of dimensions $m_y = \ell_y + 2$ and $m_q = \ell_q + 2$, meaning that once \tilde{V}^m and \tilde{V}_o^m are created at the beginning they are not enriched anymore, namely no more bases are added to them since the conditions on lines 4 and 18 of Algorithm 1 are never true. The value of $\tilde{\sigma}_y$ and $\tilde{\sigma}_q$ change significantly in the different tests, but in the end we see that they hold good approximated max efficiencies $\tilde{\eta}_y$ and $\tilde{\eta}_q$, which we can read as “efficiency estimators” for the test efficiencies $\hat{\eta}_y$ and $\hat{\eta}_q$.

We conclude with a comment on the hierarchical estimators. Even if, as we have stressed, these are just approximations of the estimators, they seem tight even with a relatively small effort: indeed, if the time of evaluation of an RB solution amounts to 5% of the time evaluating a FE solution, we can expect the time to evaluate the estimator to amount to around 10% of the time evaluating the true error (since the error estimator consists in evaluating two RB solutions).

	u_1	u_2	u_3
Time greedy	3424 s	3456 s	3704 s
Number of bases of V^ℓ, V_o^ℓ : ℓ_y, ℓ_q	8, 4	8, 4	7, 4
Number of bases of V^m, V_o^m : m_y, m_q	10, 6	10, 6	9, 6
Approximated σ 's: $\tilde{\sigma}_y, \tilde{\sigma}_q$	0.18, 0.46	0.22, 0.05	0.03, 0.67
Approx. max. efficiency $\tilde{\eta}_y, \tilde{\eta}_q$	1.20, 1.64	1.25, 1.05	1.03, 2.26
Avg. time FE	1.50 s	1.56 s	1.58 s
Avg. time RB	0.05 s	0.05 s	0.08 s
Maximum test errors: $\hat{E}_y^\ell, \hat{E}_q^\ell$	7.22e-06, 1.19e-05	6.31e-06, 2.28e-05	7.38e-06, 2.33e-05
Maximum test efficiencies: $\hat{\eta}_y, \hat{\eta}_q$	1.12, 1.36	1.18, 1.03	1.01, 1.74

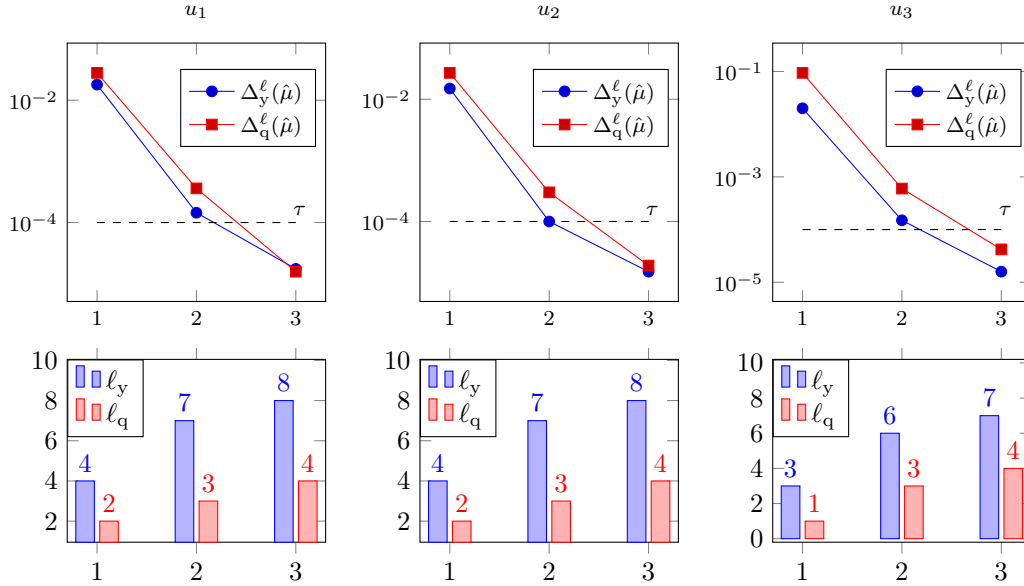
TABLE 1. Comparison of the test runs for three different control inputs u .

FIGURE 2. Visual comparison of the Greedy results for the three different control inputs. In both rows, the current greedy iteration is indicated on the x -axis: in the first row we can see how the convergence of the RB error estimators under tolerance is reached in three iterations, while in the second row we see the growing of the dimensions of the RB spaces.

5. THE PARAMETER OPTIMIZATION

Now we are interested to solve numerically the non-linear PDE-constrained parameter optimization problem

$$\min J(y, q, \boldsymbol{\mu}) \quad \text{s.t.} \quad (y, q) \in \mathcal{Y} \times \mathcal{Q} \text{ is a weak solution of (2) and } \boldsymbol{\mu} \in \mathcal{P}_{\text{ad}}. \quad (\mathbf{P})$$

Problem (6) is uniquely solvable only locally in time. For that reason, we make use of the following hypothesis.

Assumption 3. For given final time $T > 0$ there exists a unique solution pair $(y, q) \in \mathcal{Y} \times \mathcal{Q}$ to (6) for any $\boldsymbol{\mu} \in \mathcal{P}_{\text{ad}}$ which is denoted as $(y(\boldsymbol{\mu}), q(\boldsymbol{\mu}))$.

For $\mathcal{W} := L^2(0, T; H)$ the cost functional is defined as the \mathcal{W} -norm of the error between the observable function $\eta : \mathcal{Y} \times \mathcal{Q} \times \mathcal{P}_{\text{ad}} \rightarrow \mathcal{W}$ and a given data function $w \in \mathcal{W}$ that depends on $\boldsymbol{\mu}^* \in \mathcal{P}_{\text{ad}}$, the underlying

parameter, plus a regularization term. Then,

$$J(y, q, \boldsymbol{\mu}) = \frac{\alpha^J}{2} \|\eta(y, q, \boldsymbol{\mu}) - w\|_{\mathcal{W}}^2 + \frac{\lambda}{2} \|\boldsymbol{\mu} - \hat{\boldsymbol{\mu}}\|_2^2 \quad \text{for } \boldsymbol{\mu} \in \mathcal{P}_{\text{ad}}, \quad (24)$$

where $\alpha^J > 0$, $\lambda > 0$ hold and $\hat{\boldsymbol{\mu}} \in \mathcal{P}_{\text{ad}}$ is a reference parameter. Then, setting $\hat{\eta}(\boldsymbol{\mu}) := \eta(y(\boldsymbol{\mu}), q(\boldsymbol{\mu}), \boldsymbol{\mu})$, we define the reduced cost function as

$$\hat{J}(\boldsymbol{\mu}) = \frac{\alpha^J}{2} \|\hat{\eta}(\boldsymbol{\mu}) - w\|_{\mathcal{W}}^2 + \frac{\lambda}{2} \|\boldsymbol{\mu} - \hat{\boldsymbol{\mu}}\|_2^2. \quad (25)$$

In many applications including battery systems, we only have limited information and can only measure one of the two states. We assume our case to be similar, namely we can only measure the state $q(\boldsymbol{\mu})$, so that $\hat{\eta}(\boldsymbol{\mu}) = q(\boldsymbol{\mu})$. Finally, we rewrite the optimization problem in reduced form as

$$\min \hat{J}(\boldsymbol{\mu}) \quad \text{s.t.} \quad \boldsymbol{\mu} \in \mathcal{P}_{\text{ad}}. \quad (\hat{\mathbf{P}})$$

The FE and the RB approximations will be, respectively,

$$\hat{J}^h(\boldsymbol{\mu}) = \frac{\alpha^J}{2} \sum_{k=1}^K \alpha_k \|q^k(\boldsymbol{\mu}) - w^k\|_{M_q}^2 + \frac{\lambda}{2} \|\boldsymbol{\mu} - \hat{\boldsymbol{\mu}}\|_2^2$$

and

$$\hat{J}^\ell(\boldsymbol{\mu}) = \frac{\alpha^J}{2} \sum_{k=1}^K \alpha_k \|q^{k,\ell}(\boldsymbol{\mu}) - w^k\|_{M_q}^2 + \frac{\lambda}{2} \|\boldsymbol{\mu} - \hat{\boldsymbol{\mu}}\|_2^2,$$

where $\alpha_0, \dots, \alpha_K$ are the trapezoidal weights for the discretization of the temporal integral and w^k is the coordinate vector of the H -projection of

$$w^k = \frac{1}{\Delta t} \int_{t_k - \Delta t/2}^{t_k + \Delta t/2} w(s) \, ds \quad \text{for } k = 1, \dots, K \text{ and } t_k = k\Delta t$$

onto V_0 .

Remark 5.1. The evaluation of \hat{J}^ℓ is online efficient, since pre-evaluating

$$\mathbf{r}_1^k = \Psi_q^\top M_q w^k \in \mathbb{R}^{\ell_q} \quad \text{and} \quad \mathbf{r}_2^k = w^{k\top} M_q w^k \in \mathbb{R} \quad \text{for } k = 1, \dots, K,$$

then

$$\|q^{k,\ell}(\boldsymbol{\mu}) - w^k\|_{M_q}^2 = (\Psi_q \hat{q}^k(\boldsymbol{\mu}) - w^k)^\top M_q (\Psi_q \hat{q}^k(\boldsymbol{\mu}) - w^k) = \hat{q}^k(\boldsymbol{\mu})^\top M_q^\ell \hat{q}^k(\boldsymbol{\mu}) - 2\hat{q}^k(\boldsymbol{\mu})^\top \mathbf{r}_1^k + \mathbf{r}_2^k.$$

Next, we show an approximated a-posteriori error estimator for the reduced cost using the hierarchical error estimator $\Delta_q^\ell(\boldsymbol{\mu})$.

Proposition 5.2. *For all $\boldsymbol{\mu} \in \mathcal{P}_{\text{ad}}$, the following estimate on the RB error of the cost functional holds:*

$$\left| \hat{J}^h(\boldsymbol{\mu}) - \hat{J}^\ell(\boldsymbol{\mu}) \right| \leq \Delta_J^\ell(\boldsymbol{\mu}),$$

where

$$\Delta_J^\ell(\boldsymbol{\mu}) = \frac{\alpha^J L^4}{2\pi^4} \Delta_q^\ell(\boldsymbol{\mu})^2 + \frac{\alpha^J L^2}{\pi^2} \Delta_q^\ell(\boldsymbol{\mu}) \sqrt{\tilde{J}^\ell(\boldsymbol{\mu})} \quad (26)$$

and $\tilde{J}^\ell(\boldsymbol{\mu}) = \sum_{k=1}^K \alpha_k \|q^{k,\ell}(\boldsymbol{\mu}) - w^k\|_{M_q}^2$.

Proof. As a first step, the following equality holds

$$\hat{J}^h(\boldsymbol{\mu}) - \hat{J}^\ell(\boldsymbol{\mu}) = \frac{\alpha^J}{2} \sum_{k=1}^K \alpha_k (\langle \mathbf{q}^k(\boldsymbol{\mu}) - \mathbf{w}^k, \mathbf{q}^k(\boldsymbol{\mu}) - \mathbf{w}^k \rangle_{M_q} - \langle \mathbf{q}^{k,\ell}(\boldsymbol{\mu}) - \mathbf{w}^k, \mathbf{q}^{k,\ell}(\boldsymbol{\mu}) - \mathbf{w}^k \rangle_{M_q}). \quad (27)$$

Then, adding and subtracting the term $\langle \mathbf{q}^k(\boldsymbol{\mu}) - \mathbf{w}^k, \mathbf{q}^{k,\ell}(\boldsymbol{\mu}) - \mathbf{w}^k \rangle_{M_q}$ to each element in the sum in (27) we can write

$$\begin{aligned} & \langle \mathbf{q}^k(\boldsymbol{\mu}) - \mathbf{w}^k, \mathbf{q}^k(\boldsymbol{\mu}) - \mathbf{w}^k \rangle_{M_q} - \langle \mathbf{q}^{k,\ell}(\boldsymbol{\mu}) - \mathbf{w}^k, \mathbf{q}^{k,\ell}(\boldsymbol{\mu}) - \mathbf{w}^k \rangle_{M_q} \\ &= \langle \mathbf{q}^k(\boldsymbol{\mu}) - \mathbf{w}^k, \mathbf{q}^k(\boldsymbol{\mu}) - \mathbf{q}^{k,\ell}(\boldsymbol{\mu}) \rangle_{M_q} + \langle \mathbf{q}^k(\boldsymbol{\mu}) - \mathbf{q}^{k,\ell}(\boldsymbol{\mu}), \mathbf{q}^{k,\ell}(\boldsymbol{\mu}) - \mathbf{w}^k \rangle_{M_q} \\ &= \langle \mathbf{q}^k(\boldsymbol{\mu}) - \mathbf{q}^{k,\ell}(\boldsymbol{\mu}), \mathbf{q}^k(\boldsymbol{\mu}) + \mathbf{q}^{k,\ell}(\boldsymbol{\mu}) - 2\mathbf{w}^k \rangle_{M_q} \\ &= \langle \mathbf{q}^k(\boldsymbol{\mu}) - \mathbf{q}^{k,\ell}(\boldsymbol{\mu}), \mathbf{q}^k(\boldsymbol{\mu}) - \mathbf{q}^{k,\ell}(\boldsymbol{\mu}) \rangle_{M_q} + 2\langle \mathbf{q}^k(\boldsymbol{\mu}) - \mathbf{q}^{k,\ell}(\boldsymbol{\mu}), \mathbf{q}^{k,\ell}(\boldsymbol{\mu}) - \mathbf{w}^k \rangle_{M_q}. \end{aligned}$$

Hence,

$$|\hat{J}^h(\boldsymbol{\mu}) - \hat{J}^\ell(\boldsymbol{\mu})| \leq \frac{\alpha^J}{2} \sum_{k=1}^K \alpha_k \|\mathbf{q}^k(\boldsymbol{\mu}) - \mathbf{q}^{k,\ell}(\boldsymbol{\mu})\|_{M_q}^2 + \alpha^J \sum_{k=1}^K \alpha_k |\langle \mathbf{q}^k(\boldsymbol{\mu}) - \mathbf{q}^{k,\ell}(\boldsymbol{\mu}), \mathbf{q}^{k,\ell}(\boldsymbol{\mu}) - \mathbf{w}^k \rangle_{M_q}|. \quad (28)$$

Using (4), (18b) and (19) we can estimate

$$\sum_{k=1}^K \alpha_k \|\mathbf{q}^k(\boldsymbol{\mu}) - \mathbf{q}^{k,\ell}(\boldsymbol{\mu})\|_{M_q}^2 \leq c_P^2 E_q^\ell(\boldsymbol{\mu})^2 \leq c_P^2 \Delta_q^\ell(\boldsymbol{\mu})^2. \quad (29)$$

On the other hand, using the Cauchy-Schwarz inequality and (29) we get

$$\begin{aligned} & \sum_{k=1}^K \alpha_k |\langle \mathbf{q}^k(\boldsymbol{\mu}) - \mathbf{q}^{k,\ell}(\boldsymbol{\mu}), \mathbf{q}^{k,\ell}(\boldsymbol{\mu}) - \mathbf{w}^k \rangle_{M_q}| \\ & \leq \left(\sum_{k=1}^K \alpha_k \|\mathbf{q}^k(\boldsymbol{\mu}) - \mathbf{q}^{k,\ell}(\boldsymbol{\mu})\|_{M_q}^2 \right)^{1/2} \left(\sum_{k=1}^K \alpha_k \|\mathbf{q}^{k,\ell}(\boldsymbol{\mu}) - \mathbf{w}^k\|_{M_q}^2 \right)^{1/2} \leq c_P \Delta_q^\ell(\boldsymbol{\mu}) \sqrt{\tilde{J}^\ell(\boldsymbol{\mu})}. \end{aligned} \quad (30)$$

Inserting (29) and (30) into (28) we get

$$|\hat{J}^h(\boldsymbol{\mu}) - \hat{J}^\ell(\boldsymbol{\mu})| \leq \frac{\alpha^J c_P^2}{2} \Delta_q^\ell(\boldsymbol{\mu})^2 + \alpha^J c_P \Delta_q^\ell(\boldsymbol{\mu}) \sqrt{\tilde{J}^\ell(\boldsymbol{\mu})}.$$

Using $c_P = (L/\pi)^2$ the optimal Poincaré constant in $[0, L]$, we finally get (26). \square

5.1. The optimization algorithm

We solve the optimization problem $(\hat{\mathbf{P}})$ in a trust-region (TR) framework using the RB model as a surrogate model. This was done in the recent work [3, 23, 32, 34].

The TR optimization algorithm computes iteratively a first-order critical point of $(\hat{\mathbf{P}})$. At each iteration $i \geq 0$ of the optimization algorithm, a cheaply computable model $m^{(i)}$ (approximation of the reduced cost) is used to accurately represent the function \hat{J}^h in a reasonable neighborhood of $\boldsymbol{\mu}^{(i)}$, called *trust region* $\mathcal{T}(\delta^{(i)}) = \{\boldsymbol{\mu} : \|\boldsymbol{\mu} - \boldsymbol{\mu}^{(i)}\|_2 \leq \delta^{(i)}\}$, where $\delta^{(i)}$ is called *TR radius*. The TR method finds the next iteration $\boldsymbol{\mu}^{(i+1)}$ of the optimization algorithm by solving the problem

$$\min_{s \in \mathbb{R}^d} m^{(i)}(s) \quad \text{s.t.} \quad \|s\|_2 \leq \delta^{(i)}, \quad \boldsymbol{\mu}^{(i)} + s \in \mathcal{P}_{\text{ad}}. \quad (31)$$

For $\boldsymbol{\mu} = \boldsymbol{\mu}^{(i)} + s$, the RB version of (31) is

$$\min_{\boldsymbol{\mu} \in \mathcal{P}_{\text{ad}}} \hat{J}^{\ell, (i)}(\boldsymbol{\mu}) \quad \text{s.t.} \quad \mathbf{q}^{(k)}(\boldsymbol{\mu}) := \frac{\Delta_J^{\ell, (i)}(\boldsymbol{\mu})}{\hat{J}^{\ell, (i)}(\boldsymbol{\mu})} \leq \delta^{(i)}. \quad (32)$$

Here and whenever some quantity depends on the iteration i , we show it in the superscript (i) , like the RB cost $\hat{J}^{\ell, (i)}$. The ratio $q^{(i)}$ quantifies the accuracy of the RB and is used to define the TR. As we have seen in (26), the value $\Delta_J^{\ell, (i)}(\boldsymbol{\mu})$ is dependent on σ_q , which is evaluated as $\sigma_q = \sigma_q^{(i)} = E_q^m(\boldsymbol{\mu}^{(i)})^2 / E_q^\ell(\boldsymbol{\mu}^{(i)})^2$ at each iteration.

Whether the solution $\tilde{\boldsymbol{\mu}}$ of (32) is accepted as the next step of the optimization algorithm, is decided based on the error-aware sufficient decrease condition (EASDC) introduced in [34, Formula (3.9)], i.e., if

$$\hat{J}^{\ell, (i+1)}(\boldsymbol{\mu}^{(i+1)}) \leq \hat{J}^{\ell, (i)}(\boldsymbol{\mu}_{AGC}^{(i)}), \quad (33)$$

where $\boldsymbol{\mu}_{AGC}^{(i)}$ is the approximated generalized Cauchy (AGC) point, defined as the steepest descent method solution in the initial direction $-\nabla \hat{J}^{\ell, (i)}(\boldsymbol{\mu}^{(i)})$. Since $\hat{J}^{\ell, (i)}$ refers to the reduced model at iteration k , while $\hat{J}^{\ell, (i+1)}$ refers instead to the model after the $(k+1)$ -th (eventual) enrichment, the condition is not effortless to verify, and instead other similar conditions are tested, cf. [3, 23, 34].

If the candidate is rejected, we can expect the surrogate model to be not accurate enough, and hence enrich the RB models or reduce the TR radius. On the other hand, if it is accepted, we can even decide that there is no need to enrich the model, as explained in [3]. The algorithm then stops when $\|\boldsymbol{\mu}^{(i+1)} - \mathcal{P}_{\mathcal{P}_{\text{ad}}}(\boldsymbol{\mu}^{(i+1)} - \nabla \hat{J}^h(\boldsymbol{\mu}^{(i+1)}))\|_2 \leq \varepsilon_{tr}$, where $\varepsilon_{tr} = 10^{-5}$ is the overall tolerance.

Remark 5.3. Following [3,34] one can prove the convergence of our optimization method by assuming additional hypotheses. In fact, we need uniform Lipschitz continuity for the reduced cost $\hat{J}^{\ell, (k)}$, the mapping $\boldsymbol{\mu} \mapsto \mathbf{q}^{(i)}$ has to be uniformly continuous, (32) should admit at least one optimal solution satisfying (33) and the gradient of the reduced cost functional has to fulfill a so-called *Carter condition* [7]. \diamond

5.2. Numerical experiments (cont'd)

We will now show the accuracy and the speed-up of the TR optimization algorithm using the hierarchical error estimation. Let $\Omega = (0, 1)$, $T = 2$, $\kappa_1(x) \equiv \kappa_2(x) \equiv 1$, $y_o(x) \equiv 5$ and \mathcal{P}_{ad} defined as in Section 4.2. Furthermore, let $\alpha^J = 10^5$, $\lambda = 10^{-7}$, $\boldsymbol{\mu}^{(0)} = \hat{\boldsymbol{\mu}} = (3, 3, 3, 3)$ (i.e. the middle point of \mathcal{P}_{ad}) and let $u(t) = -3 \cdot \mathbf{1}_{[0, 4/3)}(t) + 3 \cdot \mathbf{1}_{[4/3, 2]}(t)$. As discretization dimensions we choose $n = 201$ (linear Lagrangian elements on 200 spatial nodes) and $K = 201$, and as data we use a virtual noisy measurement of the q state variable corresponding to the hidden parameter $\boldsymbol{\mu}^* = (2, 3, 4, 5)$, namely

$$w_j^k = q_j^k(\boldsymbol{\mu}^*) + \varepsilon_j^k, \quad \text{where } \varepsilon_j^k \sim \mathcal{N}(0, \sigma_d^2) \text{ for any } j = 1, \dots, n, \quad k = 1, \dots, K,$$

where $\sigma_d^2 = 10^{-3}$ is the simulated measurement variance.

Our computations are done in Python and the results of the TR optimization are compared with the results of the full-order (FO) optimization problem solved with the function `fmin_l_bfgs_b` from the `scipy.optimize` library. The results are shown in Table 2. The speed-up of the TR optimization algorithm in the overall CPU time is 5.3, and we can see how the number of iterations and FO evaluations are much smaller. In the last two columns we can see the norms of the absolute and relative error between the true hidden parameter and the solution of the parameter optimization algorithm, i.e. $\mathbf{e}_\mu^{\text{abs}} := \|\boldsymbol{\mu}^* - \boldsymbol{\mu}^{\text{opt}}\|_2$ and $\mathbf{e}_\mu^{\text{rel}} := \|\boldsymbol{\mu}^* - \boldsymbol{\mu}^{\text{opt}}\|_2 / \|\boldsymbol{\mu}^*\|_2$. As shown, both optimization results are accurate enough. To show the accuracy of the RB approximation, in Figure 3 the errors between the FE and RB approximations corresponding to the underlying hidden parameter $\boldsymbol{\mu}^*$ are plotted.

The speed-up given by the TR optimization, shown in Table 2 can be even higher when the speed-up given by the evaluation of the RB solution in comparison with the FE solution is higher. For example, using quadratic

	Time	Iterations	FO evaluations	e_{μ}^{abs}	e_{μ}^{rel}
FO optimization	155 s	33	40	0.028	0.0039
TR-RB	29 s	3	5	0.029	0.0039

TABLE 2. Results for $\mu^* = (2, 3, 4, 5)$ and $u(t) = -3 \cdot \mathbf{1}_{[0,4/3]}(t) + 3 \cdot \mathbf{1}_{[4/3,2]}(t)$ using linear Lagrangian elements.

Lagrangian elements (so that $n = 401$) the computational time for evaluating a FO solution is a bit higher (8 seconds) and the optimization algorithm takes longer. The results are shown in Table 3. Here the speed-up with respect to the overall CPU time is about 15, and it is reasonable to believe that for more accurate discretizations it can get even better.

	Time	Iterations	FO evaluations	e_{μ}^{abs}	e_{μ}^{rel}
FO optimization	782 s	36	41	0.016	0.0022
TR-RB	52 s	3	3	0.018	0.0025

TABLE 3. Results for $\mu^* = (2, 3, 4, 5)$ and $u(t) = -3 \cdot \mathbf{1}_{[0,4/3]}(t) + 3 \cdot \mathbf{1}_{[4/3,2]}(t)$ using quadratic Lagrangian elements.

As a further example, we simply change the hidden parameter to $\mu^* = (4, 4, 2, 1.5)$ and use linear Lagrangian elements. As we can see in Table 4, the results do not change significantly with respect to results seen in Table 2, both in the overall time and in number of iterations.

	Time	Iterations	FO evaluations	e_{μ}^{abs}	e_{μ}^{rel}
FO optimization	166 s	35	44	0.0082	0.0013
TR-RB	27 s	4	4	0.0082	0.0013

TABLE 4. Results for $\mu^* = (4, 4, 2, 1.5)$ and $u(t) = -3 \cdot \mathbf{1}_{[0,4/3]}(t) + 3 \cdot \mathbf{1}_{[4/3,2]}(t)$ using linear Lagrangian elements.

On the other hand, if we change the input u to, say, $u(t) = 0.5 \cdot \cos(10t) + 0.4 \cdot \sin(20t)$, then the hidden parameter (in this example again $\mu^* = (2, 3, 4, 5)$) is not well approximated both for the FO and the reduced-order approximations. But nonetheless, the convergence time is much faster; cf. Table 5, and the optimization algorithm falls into a local minimum much faster.

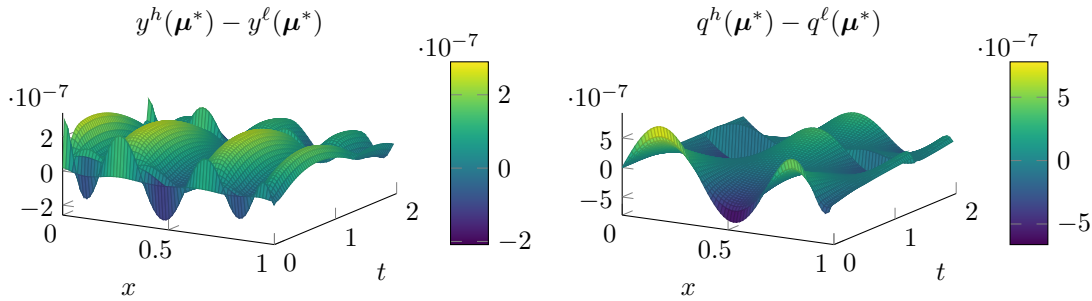


FIGURE 3. Errors between FE and RB solutions for $\mu^* = (2, 3, 4, 5)$ and $u(t) = -3 \cdot \mathbf{1}_{[0,4/3]}(t) + 3 \cdot \mathbf{1}_{[4/3,2]}(t)$ using linear Lagrangian elements.

	Time	Iterations	FO evaluations	e_{μ}^{abs}	e_{μ}^{rel}
FO optimization	45 s	12	13	1.00	0.13
TR-RB	9 s	2	3	1.00	0.13

TABLE 5. Results for $\mu^* = (2, 3, 4, 5)$ and $u(t) = 0.5 \cdot \cos(10t) + 0.4 \cdot \sin(20t)$ using linear Lagrangian elements.

6. CONCLUSIONS

In this paper, we have considered a parameter-dependent coupled elliptic-parabolic problem. First, we have proved that a unique weak solution exists locally in time for some assumptions regarding the coupling non-linearity, the parameter space, the initial condition, and the control function (cf. Assumption 1). Then, we have defined a full-order discretization, sufficiently accurate but expensive to solve. For this reason, the reduced basis (RB) approximation was defined. Due to the non-linear nature of the problem, a rigorous, online-efficient error estimate is not computable. On the other hand, we have defined approximated hierarchical error estimators for the state variables and for a pretty general quadratic cost functional.

Through a weak greedy algorithm, we have built an RB model in the whole parameter space and found approximated error estimates. Later we have shown the accuracy and efficiency of such estimates on a random set of parameters. Consequently, we have used the error estimates in a trust-region (TR) optimization framework, based on the recent work of RB-TR algorithms [3, 23, 32, 34]. The numerical results show a significant speed-up without sacrificing the accuracy of the optimized parameters.

Let us mention that our numerical experiments carried out in Section 5.2 show that the choice of the input function u influences the parameter optimization with respect to identifiability. In *optimal input design* the goal is to find the “best” input function for the parameter optimization; see, e.g., [2, 18, 24]. This is a possible future research direction; cf. [32].

A. APPENDIX

A.1. Proof of Theorem 2.2

We show the existence of the solution of (\mathbf{E}_w) by a fixed point argument, and the $C_o(\bar{\Omega})$ -estimate is obtained during the proof. For $\delta \in [0, 1]$, f.a.a. $t \in [0, T]$, given $y \in \mathcal{Y}_M^T$, $u \in \mathcal{U}_{\text{ad}}$ and $v \in C_o(\bar{\Omega})$, let us consider the equation

$$\mu_3 \int_{\Omega} \kappa_2(x) q_x(t, x) \varphi'(x) dx + \mu_4 \delta \int_{\Omega} f(y(t, x), v(x)) \varphi(x) dx = u(t) \varphi(L) \quad \text{for all } \varphi \in V_o. \quad (34)$$

F.a.a. $t \in [0, T]$ we also introduce the solution operator

$$\mathcal{T}_t : [0, 1] \times C_o(\bar{\Omega}) \rightarrow C_o(\bar{\Omega}),$$

which maps (δ, v) to $q(t)$ as the solution of (34) using $y(t)$ and $u(t)$. Then, using Leray-Schauder principle (cf., e.g., [14, p. 189]) we prove that there exists a fixed point $q(t)$ of $\mathcal{T}_t(1, \cdot) : C_o(\bar{\Omega}) \rightarrow C_o(\bar{\Omega})$ f.a.a. $t \in [0, T]$.

Wellposedness of \mathcal{T}_t : Due to the fact that $y(t) \in C(\bar{\Omega})$, $v \in C_o(\bar{\Omega})$, and that f is continuous, it can be easily be shown that $\mu_4 \delta f(y(t), v) \in C(\bar{\Omega})$. Due to Assumption 1-4) we can apply the Lax-Milgram theorem to derive the existence of a unique weak solution $q(t) \in V_o \hookrightarrow C_o(\bar{\Omega})$ to (34) satisfying

$$\|q(t)\|_{C(\bar{\Omega})} \leq c_e \|q(t)\|_{V_o} \leq c_1(M) \left(\|v\|_{C(\bar{\Omega})} + |u(t)| \right), \quad (35)$$

where the constant $c_1(M)$ does not depend on v , $y(t)$ or $u(t)$ but it does depend on M .

Continuity of $\mathcal{T}_t(\delta, \cdot) : C_o(\overline{\Omega}) \rightarrow C_o(\overline{\Omega})$ for any $\delta \in [0, 1]$: For any $v_1, v_2 \in C_o(\overline{\Omega})$ we set $q_1(t) := \mathcal{T}_t(\delta, v_1)$ and $q_2(t) := \mathcal{T}_t(\delta, v_2)$. Due to (3) and $\mu \in \mathcal{P}_{ad}$ we can write that

$$\begin{aligned} \|q_1(t) - q_2(t)\|_{C(\overline{\Omega})} &\leq c_e \|q_1(t) - q_2(t)\|_{V_o} \\ &\leq c_2 \delta \left(\|f(y(t), v_1) - f(y(t), v_2)\|_{C(\overline{\Omega})} \right) \\ &\leq c_3(M) \left(\|\sinh(v_1) - \sinh(v_2)\|_{C(\overline{\Omega})} \right), \end{aligned}$$

where c_2 and $c_3(M)$ do not depend on $y(t)$, v or $u(t)$. Thus the claims follow by the continuity of \sinh .

Uniform continuity of $\mathcal{T}_t(\cdot, v) : [0, 1] \rightarrow C_o(\overline{\Omega})$ on any bounded set $\mathcal{C} \subset C_o(\overline{\Omega})$: Let $\delta_1, \delta_2 \in [0, 1]$. Then for $q_1(t) = T(\delta_1, v)$ and $q_2(t) = T(\delta_2, v)$ we have

$$\begin{aligned} \|q_1(t) - q_2(t)\|_{C(\overline{\Omega})} &\leq c_e \|q_1(t) - q_2(t)\|_{V_o} \\ &\leq c_4 |\delta_1 - \delta_2| \|f(y(t), v)\|_{L^\infty(\Omega)} \\ &\leq c_5(M) |\delta_1 - \delta_2| \|\sinh(v)\|_{L^\infty(\Omega)}, \end{aligned}$$

where c_4 and $c_5(M)$ do not depend on $y(t)$, v or $u(t)$. Since $\|\sinh(v)\|_{C(\overline{\Omega})}$ is uniformly bounded on the bounded set $\mathcal{C} \subset C_o(\overline{\Omega})$, the operator $\mathcal{T}_t(\cdot, v) : [0, 1] \rightarrow C_o(\overline{\Omega})$ is uniformly continuous on \mathcal{C} .

Compactness of $\mathcal{T}_t(\delta, \cdot)$ for any $\delta \in [0, 1]$: This follows from the fact that for every $\delta \in [0, 1]$ the operator $\mathcal{T}_t(\delta, \cdot) : C_o(\overline{\Omega}) \rightarrow V_o$ is continuous and the space V_o is compactly embedded in $C_o(\overline{\Omega})$ (see, e.g., [38, Theorem 7.97]).

Uniform boundedness of $q(t)$ satisfying $\mathcal{T}_t(\delta, q(t)) = q(t)$ for any $\delta \in [0, 1]$: Let an arbitrary $\delta \in [0, 1]$ be given and let us test (34) with $\varphi = q(t)$. Then, we get

$$\mu_3 \int_{\Omega} \kappa_2(x) |q_x(t, x)|^2 dx + \mu_4 \delta \int_{\Omega} f(y(t, x), q(t, x)) q(t, x) dx = q(t, L) u(t).$$

Using $y \in \mathcal{Y}_M^T$ and the fact that $\sinh(q)q \geq q^2$ for any $q \in \mathbb{R}$, we obtain that

$$\mu_{a,3} \kappa_a \|q_x(t)\|_H^2 + \mu_4 \delta \sqrt{1/M} \|q(t)\|_H^2 \leq |q(t, L)| |u(t)|.$$

Hence, since $|q(t, L)| \leq \|q(t)\|_{V_o}$ and using (3), Young's inequality, we get the estimate (10), namely

$$\|q(t)\|_{V_o} \leq c(M) |u(t)| \leq c(M) c_u,$$

where $c(M)$ does not depend on q or on δ .

Uniqueness of the solution of $\mathcal{T}_t(0, q(t)) = q(t)$ in $C_o(\overline{\Omega})$: This follows from the fact that for $\delta = 0$ problem (34) is linear and well-posed.

Application of Leray-Schauder principle : Having satisfied all of the hypotheses of the Leray-Schauder principle, the existence of a fixed point $T(1, q(t)) = q(t)$ in $C_o(\overline{\Omega})$ follows.

Uniqueness : Consider $q_1(t) = \mathcal{T}_t(1, q_1(t))$, $q_2(t) = \mathcal{T}_t(1, q_2(t))$ and let $\bar{q}(t) = q_1(t) - q_2(t)$. From (34) we can get

$$\mu_3 \int_{\Omega} \kappa_2 \bar{q}_x(t) \varphi' dx + \mu_4 \int_{\Omega} (f(y(t), q_1(t)) - f(y(t), q_2(t))) \varphi dx = 0 \quad \text{for all } \varphi \in V_o.$$

Choosing $\varphi = \bar{q}(t)$, we get

$$\mu_3 \int_{\Omega} \kappa_2(x) |\bar{q}_x(t)|^2 dx + \mu_4 \int_{\Omega} (f(y(t), q_1(t)) - f(y(t), q_2(t))) \bar{q}(t) dx = 0.$$

Using the mean value theorem (f is continuously differentiable with respect to the variable q), we get

$$f(y(t, x), q_1(t, x)) - f(y(t, x), q_2(t, x)) = \partial_q f(y(t, x), \xi(t, x)) \bar{q}(t, x) \quad \text{f.a.a. } (t, x) \in Q_T$$

for some $\xi(t, x)$ between $q_1(t, x)$ and $q_2(t, x)$. It follows that

$$\mu_3 \int_{\Omega} \kappa_2(x) |\bar{q}_x(t)|^2 dx + \mu_4 \int_{\Omega} \partial_q f(y(t), \xi(t)) |\bar{q}(t)|^2 dx = 0 \quad \text{f.a.a. } (t) \in [0, T].$$

By Assumption 2 the value $y(t, x)$ is positive in Q_T . Thus,

$$\partial_q f(y(t), \xi(t)) = \sqrt{y(t, x)} \cosh(\xi(t, x)) \geq 0 \quad \text{a.e. in } Q_T.$$

Utilizing $\kappa_2 \geq \kappa_a > 0$ on Ω we infer that $\bar{q}_x = 0$ a.e. in Q_T . Due to $\bar{q} \in V_{\circ}$ f.a.a. $t \in [0, T]$ we have $\bar{q} = 0$ a.e. in Q_T , which implies the uniqueness.

A.2. Proof of Theorem 2.3

The proof proceeds with the fixed point argument using Schauder's fixed point theorem [16, Theorem 11.1 and Corollary 11.2]. In this case, we consider the following linear parabolic equation for a given $v \in \mathcal{Y}_M^T$ and $q \in \mathcal{Q}^T$ f.a.a. $t \in [0, T]$

$$\begin{cases} y_t(t, x) - \mu_1 (\kappa_1(x) y_x(t, x))_x = \mu_2 f(v(t, x), q(t, x)) & \text{f.a.a. } (t, x) \in Q_T, \\ y_x(t, 0) = y_x(t, L) = 0 & \text{f.a.a. } t \in (0, T], \\ y(0, x) = y_{\circ}(x) & \text{f.a.a. } x \in \Omega. \end{cases} \quad (36)$$

It is well known that for $w = (v, q) \in \mathcal{Y}_M^T \times \mathcal{Q}^T$, there exists a unique *weak solution* $y \in W(0, T; V, V')$ to (36) satisfying $y(0) = y_{\circ}$ in H and

$$\frac{d}{dt} \langle y(t), \varphi \rangle_H + \mu_1 \hat{a}^1(y(t), \varphi) = \mu_2 \hat{g}^1(w(t), \varphi) \quad \text{for all } \varphi \in V \text{ and f.a.a. } t \in (0, T]. \quad (37)$$

Further, for $y_{\circ} \in V$, this solution is even more regular and it belongs to the space $W(0, T; E, H)$ with

$$E := \{u \in H^2(\Omega) = H^2(0, L) : u_x(0) = u_x(L) = 0\}.$$

In this case, due to the continuous embeddings $E \hookrightarrow V \hookrightarrow H$, we have $W(0, T; E, H) \hookrightarrow C([0, T]; V)$ and with standard energy estimates it can be shown that

$$\|y\|_{C([0, T]; V)}^2 + \|y\|_{L^2(0, T; H^2(\Omega))}^2 \leq c_1 e^{c_2 T} \left(\|y_{\circ}\|_V^2 + \|f(v, q)\|_{L^2(0, T; H)}^2 \right), \quad (38)$$

where c_1 and c_2 depend only on L , μ_1 , and μ_2 . See, e.g., [13, p. 382]).

Now, we define the mapping $\mathcal{T} : \mathcal{Y}_M^T \rightarrow W(0, T; E, H)$, where $y = \mathcal{T}(v)$ as the solution to (37) for any given $v \in \mathcal{Y}_M^T$. Next we show that the mapping $\mathcal{T} : \mathcal{Y}_M^{T_{\circ}} \rightarrow \mathcal{Y}_M^{T_{\circ}}$ for a suitable $T_{\circ} \in (0, T]$ is well-defined. Let $w = (v, q) \in \mathcal{Y}_M^T \times \mathcal{Q}^T$. Since $v \in \mathcal{Y}_M^T$ and $q \in \mathcal{Q}^T$, it follows that

$$\mathfrak{f}(t, x) := \mu_2 f(v(t, x), q(t, x)) \in L^2(0, T; H) \simeq L^2(Q_T).$$

We write $y = \phi + \psi$, where ϕ and ψ are the solution, respectively to

$$\begin{cases} \phi_t(t, x) - \mu_1 (\kappa_1(x) \phi_x(t, x))_x = \mathfrak{f}(t, x) & \text{f.a.a. } (t, x) \in Q_T, \\ \phi_x(t, 0) = \phi_x(t, L) = 0 & \text{f.a.a. } t \in (0, T], \\ \phi(0, x) = 0 & \text{f.a.a. } x \in \Omega. \end{cases} \quad (39)$$

and

$$\begin{cases} \psi_t(t, x) - \mu_1 (\kappa_1(x) \psi_x(t, x))_x = 0 & \text{f.a.a. } (t, x) \in Q_T, \\ \psi_x(t, 0) = \psi_x(t, L) = 0 & \text{f.a.a. } t \in (0, T], \\ \psi(0, x) = y_o & \text{f.a.a. } x \in \Omega. \end{cases} \quad (40)$$

Then, on the one hand for ϕ we can derive the estimate

$$\|\phi\|_{C([0, T]; V)} + \|\phi\|_{L^2(0, T; H^2(\Omega))} \leq c_1 e^{c_2 T} \|f\|_{L^2(0, T; H)} \quad (41)$$

with positive constants c_1 and c_2 depending only on \mathcal{P}_{ad} , κ and Ω , while on the other hand using the fact that $y_o(x) \in [2/M, M/2]$ for every $x \in \Omega$, and the comparison principle [39, A.1 Theorem and A.2 Corollary], we can conclude that

$$\psi(t, x) \in \left[\frac{2}{M}, \frac{M}{2} \right] \quad \text{f.a.a. } (t, x) \in [0, T] \times \Omega. \quad (42)$$

Furthermore, for a given $T > 0$, using $y = \psi + \phi$, (41) and (42), we can write f.a.a. $(t, x) \in [0, T] \times \Omega$ that

$$\begin{aligned} y(t, x) &\leq \frac{M}{2} + \phi(t, x) \leq \frac{M}{2} + \hat{c} e^{c_2 T} \|f\|_{L^2(0, T; H)}, \\ y(t, x) &\geq \frac{2}{M} + \phi(t, x) \geq \frac{2}{M} - \hat{c} e^{c_2 T} \|f\|_{L^2(0, T; H)}, \end{aligned} \quad (43)$$

where \hat{c} depend only on \mathcal{P}_{ad} , κ_a and Ω . Since the function $[0, T] \ni t \mapsto \gamma(t) = \hat{c} e^{c_2 t} \|f\|_{L^2(0, t; H)}$ is positive, increasing in t , and satisfies $\gamma(0) = 0$, we can find $T_o \in (0, T]$ such that

$$\hat{c}_1 e^{c_2 t} \|f\|_{L^2(0, t; H)} \leq \min \left\{ \frac{M}{2}, \frac{1}{M} \right\} \quad \text{for all } t \in [0, T_o]. \quad (44)$$

Finally, using (43) and (44) and applying Remark 2.4, we get

$$\begin{aligned} y(t, x) &\leq y_o(x) + \frac{M}{2} \leq \frac{M}{2} + \frac{M}{2} = M && \text{for all } (t, x) \in [0, T_o] \times \Omega, \\ y(t, x) &\geq y_o(x) - \frac{1}{M} \geq \frac{2}{M} - \frac{1}{M} = \frac{1}{M} && \text{for all } (t, x) \in [0, T_o] \times \Omega, \end{aligned}$$

which implies that $y \in \mathcal{Y}_M^{T_o}$ holds.

Next, we show that the mapping \mathcal{T} is continuous. Beforehand, we show that for given $v_1, v_2 \in \mathcal{Y}_M^T$, there exists $\gamma \geq 0$ such that

$$\|f(v_1, q) - f(v_2, q)\|_{L^\infty(0, T; H)} \leq \gamma \|v_1 - v_2\|_{L^\infty(0, T; H)}. \quad (45)$$

holds. We observe that f.a.a. $t \in [0, T]$

$$\begin{aligned} \|f(v_1(t), q(t)) - f(v_2(t), q(t))\|_H^2 &= \int_\Omega |f(v_1(t, x), q(t, x)) - f(v_2(t, x), q(t, x))|^2 dx \\ &= \int_\Omega \left| (\sqrt{v_1(t, x)} - \sqrt{v_2(t, x)}) \sinh(q(t, x)) \right|^2 dx, \end{aligned} \quad (46)$$

From (3) and (10) it follows that

$$\max_{x \in \Omega} |\sinh(q(t, x))| \leq \sinh \left(\|q(t)\|_{C(\bar{\Omega})} \right) \leq \sinh \left(c_e \|q(t)\|_{V_o} \right) \leq c_3(M) \quad \text{f.a.a. } t \in [0, T],$$

for a constant $c_3(M) > 0$ independent of time. Thus, using (46), we can write f.a.a. $t \in [0, T]$ that

$$\begin{aligned} \|f(v_1(t), q(t)) - f(v_2(t), q(t))\|_H^2 &\leq c_3(M)^2 \int_{\Omega} \left| \sqrt{v_1(t, x)} - \sqrt{v_2(t, x)} \right|^2 dx \\ &= c_3(M)^2 \int_{\Omega} \left| \frac{v_1(t, x) - v_2(t, x)}{\sqrt{v_1(t, x)} + \sqrt{v_2(t, x)}} \right|^2 dx \\ &\leq \gamma(M) \int_{\Omega} |v_1(t, x) - v_2(t, x)|^2 dx. \end{aligned}$$

Therefore, (45) holds for a constant $\gamma(M) > 0$ independent of v_1, v_2 and T . Using the similar estimate as in (38) and (45), we can write for every $v_1, v_2 \in \mathcal{Y}_M^T$ that

$$\|\mathcal{T}(v_1) - \mathcal{T}(v_2)\|_{C([0, T]; V)}^2 \leq c_1 e^{c_2 T} \left(\|f(v_1, q) - f(v_2, q)\|_{L^2(0, T; H)}^2 \right) \leq T \gamma^2 c_1 e^{c_2 T} \left(\|v_1 - v_2\|_{L^\infty(0, T; H)}^2 \right). \quad (47)$$

Together with (3) we get

$$\begin{aligned} \|\mathcal{T}(v_1) - \mathcal{T}(v_2)\|_{C([0, T]; C(\bar{\Omega}))}^2 &\leq c_e^2 \|\mathcal{T}(v_1) - \mathcal{T}(v_2)\|_{C([0, T]; V)}^2 \leq c_e^2 T \gamma^2 c_1 e^{c_2 T} \left(\|v_1 - v_2\|_{L^\infty(0, T; H)}^2 \right) \\ &\leq \underbrace{[L c_e^2 T \gamma^2 c_1 e^{c_2 T}]}_{=: \varrho(T)} \|v_1 - v_2\|_{C(\bar{Q}_T)}^2 = \varrho(T) \|v_1 - v_2\|_{C(\bar{Q}_T)}^2. \end{aligned}$$

Thus, we are shown that \mathcal{T} is continuous.

In order to be able to use Schauder's fixed point theorem, it remains only to show that \mathcal{T} is compact. To show this, we use the fact the solution of (36) belongs to $W(0, T; E, H)$. Due to [1, Theorem 5.2], this space is compactly embedded in $C([0, T]; H^{2\theta}(\Omega))$ for $0 < \theta < \frac{1}{2}$. Further, invoking [42, Proposition 4.3], $C([0, T]; H^{2\theta}(\Omega))$ is continuously embedded in $C(\bar{Q}_T)$ for $\theta > \frac{1}{4}$. Thus, choosing $\theta \in (\frac{1}{4}, \frac{1}{2})$, we can infer that $W(0, T; E, H)$ is compactly embedded in $C(\bar{Q}_T)$ and, thus, \mathcal{T} is compact.

Acknowledgement. We would like to thank Tim Keil (University of Münster, Germany) for fruitful discussions regarding the adaptive TR method.

REFERENCES

- [1] H. Amann. Compact embeddings of vector-valued Sobolev and Besov spaces. *Glas. Mat. Ser. III*, 35(55)(1):161–177, 2000.
- [2] A.C. Atkinson, A.N. Donev, and R.D. Tobias. *Optimum experimental designs, with SAS*, volume 34 of *Oxford Statistical Science Series*. Oxford University Press, Oxford, 2007.
- [3] S. Banholzer, T. Keil, L. Mechelli, M. Ohlberger, F. Schindler, and S. Volkwein. An adaptive projected Newton non-conforming dual approach for trust-region reduced basis approximation of PDE-constrained parameter optimization. *Pure and Applied Functional Analysis*, 7:1561–1596, 2022.
- [4] S. Banholzer, L. Mechelli, and S. Volkwein. A trust region reduced basis Pascoletti-Serafini algorithm for multi-objective PDE-constrained parameter optimization. *Mathematical and Computational Applications*, 27:39, 2022.
- [5] R.E. Bank and R.K. Smith. A posteriori error estimates based on hierarchical bases. *SIAM Journal on Numerical Analysis*, 30:921–935, 1993.
- [6] M. Barrault, Y. Maday, N.C. Nguyen, and A.T. Patera. An empirical interpolation method: application to efficient reduced-basis discretization of partial differential equations. *Comptes Rendus Mathematique*, 339, 2004.
- [7] R.G. Carter. On the global convergence of trust region algorithms using inexact gradient information. *SIAM Journal on Numerical Analysis*, 28:251–265, 1991.
- [8] S. Chaturantabut and D.C. Sorensen. Nonlinear model reduction via discrete empirical interpolation. *SIAM Journal on Scientific Computing*, 32:2737–2764, 2010.
- [9] J.R. Cho and J.T. Oden. A priori modeling error estimates of hierarchical models for elasticity problems for plate- and shell-like structures. *Mathematical and Computer Modelling*, 23:117–133, 1996.

- [10] R. Dautray and J.L. Lions. *Mathematical Analysis and Numerical Methods for Science and Technology. Volume 5 Evolution Problems I*. Springer, Berlin, Heidelberg, 2000.
- [11] C. Domínguez, E.P. Stephan, and M. Maischak. A fe-be coupling for a fluid-structure interaction problem: hierarchical a posteriori error estimates. *Numerical Methods for Partial Differential Equations*, 28:1417–1439, 2012.
- [12] M. Doyle, T.F. Fuller, and J. Newman. Modeling of galvanostatic charge and discharge of the lithium/polymer/insertion cell. *Journal of The Electrochemical Society*, 140:1256–1533, 1993.
- [13] L.C. Evans. *Partial Differential Equations*. Graduate Studies in Mathematics. American Mathematical Society, Providence, Rhode Island, 2010.
- [14] A. Friedman. *Partial Differential Equations of Parabolic Type*. Prentice-Hall, Inc., Englewood Cliffs, N.J., 1964.
- [15] T.F. Fuller, M. Doyle, and J. Newman. Simulation and optimization of the dual lithium ion insertion cell. *Journal of The Electrochemical Society*, 141:1–10, 1994.
- [16] D. Gilbarg and N.S. Trudinger. *Elliptic partial differential equations of second order*, volume 224 of *Grundlehren der mathematischen Wissenschaften [Fundamental Principles of Mathematical Sciences]*. Springer-Verlag, Berlin, second edition, 1983.
- [17] P.M. Gomadam, J.W. Weidner, R.A. Dougal, and R.E. White. Mathematical modeling of lithium-ion and nickel battery systems. *Journal of Power Sources*, 110:267–284, 2002.
- [18] Graham C. Goodwin and Robert L. Payne. *Dynamic system identification*, volume 136 of *Mathematics in Science and Engineering*. Academic Press, Inc. [Harcourt Brace Jovanovich, Publishers], New York-London, 1977. Experiment design and data analysis.
- [19] M.A. Grepl and A.T. Patera. A posteriori error bounds for reduced-basis approximations of parametrized parabolic partial differential equations. *M2AN Math. Model. Numer. Anal.*, 39(1):157–181, 2005.
- [20] B. Haasdonk. Convergence rates of the POD-greedy method. *ESAIM Math. Model. Numer. Anal.*, 47(3):859–873, 2013.
- [21] S. Hain, M. Ohlberger, M. Radic, and K. Urban. A hierarchical a posteriori error estimator for the reduced basis method. *Advances in Computational Mathematics*, 45:2191–2214, 2019.
- [22] J.S. Hesthaven, G. Rozza, and B. Stamm. *Certified Reduced Basis Methods for Parametrized Partial Differential Equations*. SpringerBriefs in Mathematics. Springer, Cham, 2016.
- [23] T. Keil, L. Mechelli, M. Ohlberger, F. Schindler, and S. Volkwein. A non-conforming dual approach for adaptive trust-region reduced basis approximation of PDE-constrained parameter optimization. *ESAIM Math. Model. Numer. Anal.*, 55(3):1239–1269, 2021.
- [24] S. Körkel, E. Kostina, H.G. Bock, and Johannes P. Schlöder. Numerical methods for optimal control problems in design of robust optimal experiments for nonlinear dynamic processes. *Optim. Method. Softw.*, 19:327–338, 2004.
- [25] K. Kunisch and S. Volkwein. Galerkin proper orthogonal decomposition methods for parabolic problems. *Numerische Mathematik*, 90(1):117–148, 2001.
- [26] O. Lass and S. Volkwein. POD Galerkin schemes for nonlinear elliptic-parabolic systems. *SIAM Journal on Scientific Computing*, 35(3):A1271–A1298, 2013.
- [27] A. Latz and J. Zausch. Thermodynamic consistent transport theory of li-ion batteries. *Journal of Power Sources*, 196(1):3296–3302, 2011.
- [28] A. Latz, J. Zausch, and O. Iliev. Modeling of species and charge transport in li-ion batteries based on non-equilibrium thermodynamics. In I. Dimov, S. Dimova, and N. Kolkovska, editors, *Numerical Methods and Applications*, pages 329–337, Berlin, Heidelberg, 2011. Springer Berlin Heidelberg.
- [29] X. Li, M. Xiao, and S.Y. Choe. Reduced order model (ROM) of a pouch type lithium polymer battery based on electrochemical thermal principles for real time applications. *Numerische Mathematik*, 90(1):117–148, 2001.
- [30] John S Newman. *Electrochemical systems*. Englewood Cliffs: Prentice Hall, 1973.
- [31] M. Ohlberger, S. Rave, and F. Schindler. *Model reduction for multiscale lithium-ion battery simulation*, volume 112, pages 317–331. Springer, Cham, 2016.
- [32] A. Petrocchi, M.K. Scharrer, and S. Volkwein. Trust-region RB methods for PDE-constrained optimization and optimal input design. *IFAC-PapersOnLine*, 55(26):149–154, 2022. 4th IFAC Workshop on Control of Systems Governed by Partial Differential Equations CPDE 2022.
- [33] P. Popov, Y. Vutov, S. Margenov, and O. Iliev. Finite volume discretization of equations describing nonlinear diffusion in li-ion batteries. In I. Dimov, S. Dimova, and N. Kolkovska, editors, *Numerical Methods and Applications*, pages 338–346. Springer Berlin Heidelberg, 2011.
- [34] E. Qian, M. Grepl, K. Veroy, and K. Willcox. A certified trust region reduced basis approach to PDE-constrained optimization. *SIAM J. Sci. Comput.*, 39(5):S434–S460, 2017.
- [35] A. Quarteroni. *Numerical models for differential problems*, volume 16 of *MS&A. Modeling, Simulation and Applications*. Springer, Cham, third edition, 2017.
- [36] A. Quarteroni, A. Manzoni, and F. Negri. *Reduced Basis Methods for Partial Differential Equations: An Introduction*. UNITEXT – La Matematica per il 3+2. Springer, Cham, 2016.
- [37] A.M. Ramos. On the well-posedness of a mathematical model for lithium-ion batteries. *Applied Mathematical Modelling*, 40:115–125, 2016.

- [38] S. Salsa. *Partial Differential Equations in Action. From Modelling to Theory*. Universitext. Springer Cham, third edition, 2016.
- [39] E. J. P. Georg Schmidt. Boundary control for the heat equation with nonlinear boundary condition. *J. Differ. Equations*, 78(1):89–121, 1989.
- [40] T. Seger. *Elliptic-Parabolic Systems with Applications to Lithium-Ion Battery Models*. PhD thesis, University of Konstanz, 2013. See <http://nbn-resolving.de/urn:nbn:de:bsz:352-241413>.
- [41] K. Smith and C.Y. Wang. Power and thermal characterization of a lithium- ion battery pack for hybrid-electric vehicles. *Journal of Power Sources*, 160:662–673, 2006.
- [42] M.E. Taylor. *Partial differential equations I. Basic theory*, volume 115 of *Applied Mathematical Sciences*. Springer, New York, second edition, 2011.
- [43] S. Volkwein and A. Wesche. The reduced basis method applied to transport equations of a lithium-ion battery. *The International Journal for Computation and Mathematics in Electrical and Electronic Engineering*, 32:1760–1772, 2013.
- [44] J. Wu, J. Xou, and H. Zou. On the well-posedness of a mathematical model for lithium-ion battery systems. *Methods and Applications of Analysis*, 13:275–298, 2006.